UNIVERSITY OF TWENTE.

**Faculty of Electrical Engineering,
Mathematics & Computer Science**

Noise-based Frequency Offset Modulation Simulation Model Design

For the analysis of Transmit-Reference Medium Access Control in Multiple Access Ad-hoc Wireless Sensor Networks

Mike Kriele

M.Sc. Thesis
January 2018

Supervisors:
prof. dr. ir. G.J. Heijenk
prof. dr. ir. F.B.J. Leferink
dr. ir. A. Meijerink
dr. ir. P.T. de Boer
I. Bilal, M.Sc.

Telecommunication Engineering Group &
Design and Analysis of Communication Systems Group
Faculty of Electrical Engineering,
Mathematics and Computer Science
University of Twente
P.O. Box 217
7500 AE Enschede
The Netherlands

Summary

The increasing use of wireless devices has led to more need for energy-efficient communication schemes. Recently, more effort have been put in researching low-power spread spectrum as an energy-efficient method of communication. transmitted reference (TR) is a low-power spread-spectrum technique which was introduced as a promising communication scheme used in short-range transmissions, such as wireless sensor networks. In TR modulation the transmitter sends the information signal along with the spreading signal shifted by a time or frequency offset, which can be demodulated by the receiver by applying the same offset. This simplifies the receiver architecture significantly. The receiver does thus not need to know the spreading signal used, allowing for any kind of spreading signal; including noise, giving birth to noise-based frequency-offset modulation (N-FOM).

N-FOM uses pure noise as information bearer. This is advantageous as it is easy to generate and eliminates the need for complex schemes for flattening the spectrum of the transmitted signal. Therefore, N-FOM allows for multiple-access communication by varying the frequency offset used in the receiver. However, due to the self-correlation module in the receiver, mixing terms of possible other concurrent active nodes increase the noise roughly quadratically; limiting the number of possible concurrent active links as bit error rates worsen.

Introducing a medium access control (MAC) protocol to regulate the number of concurrent transmissions could assist in overcoming this barier. Transmitted-Reference MAC (TR-MAC) is a protocol specifically designed to work with N-FOM. The protocol regulates the frequency offsets allocated to transmitting nodes and synchronized with them providing each transmitter a non-overlapping transmission opportunity to send packets. This in order to prevent collisions due to frequency offsets selected twice and to reduce too many concurrent active links. The protocol allows both transmitter-driven and receiver-driven communication. Although proven functional, TR-MAC has only been tested with abstractions of the physical layer and hard limits set on the number of concurrent active links. The creation of a new model is required that is not based on hard limits, but rather implements real physical-layer phenomena of the N-FOM physical layer. This in order to test how the physical layer

affects the medium access layer in ways that have previously not been accounted for.

Based on theTR-MAC simulation model as a starting point, the N-FOM physical layer has been implemented. Physical layer abstractions and hard limits have been removed. A mathematical expression of the N-FOM layer has been used to model the physical layer for simulation. In order to model a more realistic channel, a Bernoulli random process has been implemented for packet error generation to determine packet error probabilities. Simulations have been performed to verify the physical layer to test its limitations and to see the effects on MAC level in a multiple-access environment.

Results show that physical layer simulation in a single-link environment is according to theory. Simulation results follow the theoretical curve on a 99.9% confidence interval. It can thus be assumed the physical layer is implemented according to theory. Furthermore, the limitation of the physical layer was tested. For this test, nodes were put at an equal distance and made increasingly concurrently active. It became evident the physical limit, based on the parameters set, allowed for a maximum of three concurrent active links as a maximum; thus requiring the need for a MAC protocol. Multiple access simulation of the physical layer in conjunction with the MAC protocol has shown the physical layer has significant impact on the throughput of the system. The self-correlating receiver introduces mixing terms that result in a nearly quadratic increase in noise, resulting in saturation of the throughput when the number of active links increases and eventually a decay due to channel contention. The resulting throughput is less than previously resulted from the TR-MAC measurement results due to these mixing terms.

Based on the simulation results it can thus be concluded the physical layer has impact on the MAC layer that has previously been unaccounted for. Additional noise terms introduced by the self-correlation receiver have significant impact on the throughput on the system. However, it is shown that the simulator is functional and can be used further to more extensively test the system as a whole. Currently measurements performed were primarily for functionality analysis purposes, and not for practical implementation as only line-of-sight measurements have been performed. Multipath effects still have to be simulated as they did not fall within the scope of this thesis. Additionally the inclusion of a more extensive clear channel assessment state and/or channel coding could improve the system significantly.

Contents

List of acronyms

ACK	acknowledgement
AWGN	additive white Gaussian noise
BER	bit error rate
CCA	clear channel assessment
CI	confidence interval
CNR	carrier-to-noise ratio
DACS	Design and Analysis of Communication Systems
EDR	effective dynamic range
FSPL	free-space path loss
IC	integrated circuit
ICD	interated circuit design
IDF	integrate-and-dump filter
LO	local oscillator
LOS	line of sight
MA	multiple access
MAC	medium access control
MP	multi-path
N-FOM	noise-based frequency-offset modulation
NF	noise figure
PN	pseudo-noise

PSD power spectral density

RF radio frequency

S-Aloha Slotted Aloha

SNR signal-to-noise ratio

SS spread spectrum

TE Telecommunication Engineering

TR transmitted reference

TR-MAC Transmitted-Reference MAC

UWB ultra wideband

WALNUT Wireless Ad-hoc Links using robust Noise-based Ultra-wideband Transmission

WSN wireless sensor network

Chapter 1

Introduction

1.1 Motivation

With the increasing use of wireless sensor devices over the past decade and an expected exponential increase of usage of such devices over the next decade [1], the need for better energy-efficient communication schemes has been imminent. Among other things this has led to more research in low-power spread-spectrum (SS) techniques [2]–[5] as an energy-efficient method of communication. SS signals are defined as low power spectral density (PSD) signals that use radio frequency (RF) signal bandwidths that greatly exceed the minimum bandwidth required to transmit their data. The signal's spectrum is thus spread over a significantly wider RF channel than needed to transmit the information signal [6], where the ratio between the transmission bandwidth and the bandwidth of the information signal is defined as the processing gain. As SS systems are mostly designed to overlay on top of other radio systems, having a large processing gain can assist in providing robustness against interference. However, receiver signal acquisition can be challenging in SS systems with large processing gains, de-spreading is not activated prior to synchronization and the received signal has to be retrieved at very low signal-to-noise ratio (SNR) levels. This is due to the fact that in SS the PSD is low and more powerful interferers are present. Additionally, in order to make SS robust against multi-path fading, complex receiver structures have to be used [5], [7]–[11], resulting in longer acquisition times.

In wireless sensor networks (WSNs) nodes often have strict power limitations imposed due to a limited lifetime. As the battery drains, these nodes are often considered expired. The transmission and reception times of these nodes thus play an important role in their overall lifetime. As nodes are often expected to run for years (or even decades), timing plays an important role in the overall system performance of a WSN. Nodes are only allowed to wake up for short durations to transmit or receive their data. Furthermore, simple and low-cost systems are often desired. In the

case of standard ultra wideband (UWB) SS transmission, it would be difficult to compactly design energy-efficient receivers that demodulate the received signal without knowing the spreading information used at the transmitter, yet still fulfill the demanding requirements set for WSNs. Complex receiver structures, e.g. rake receivers, are often required to cope with multipath effects, resulting in increased uptimes – due to slow synchronization because of finger tuning – and battery consumption; therefore significantly reducing a node's lifetime. TR, however, could put less stress on these requirements.

Transmitted reference (TR), a slight adaption of the original SS scheme where the transmitter sends the spreading signal along with the spread information signal [12], [13], is more suitable as faster synchronization times can be achieved. An important property of TR is that complex receiver structures requiring sub-receivers to counter multipath fading, e.g. Rake receiver fingers that are tuned to a different multipath component per finger, can be omitted as the spreading signal is no longer generated in the receiver. In the case of TR the transmitter transmits a time- or frequency-shifted version of the spreading signal together with the information signal [12], [13]. This simplifies the receiver architecture to a great extent. Extracting the information signal from the spread signal requires the receiver to only know the offset used. The advantage of this approach is that the receiver does not need to generate the spreading signal used, reducing synchronization times and therefore making TR viable for low duty-cycle applications, e.g. wireless sensor devices. This also allows for noise as a reference signal, resulting in noise-based frequency-offset modulation (N-FOM). Using noise as a reference is preferable, as it is relatively easy to generate a flat additive white Gaussian noise (AWGN) spectrum and not too costly in implementation in comparison to pseudo-noise (PN) sequences or pulse positition dithering that is normally used as reference.

Furthermore, given that wireless sensor devices often operate in a WSN, multiple access (MA) is an important aspect of WSN communication. With N-FOM, having MA is easily achieved by simply adjusting the offsets used in each transmitter for different communication links. However, offsets have to be selected carefully and the possible number of simultaneous transmissions is limited, as having too many concurrent transmissions contributes to the overall noise due to cross-mixing in the receiver, leading to unacceptable bit error rates (BERs) [14]. Using an N-FOM-tailored medium access control (MAC) protocol could assist in organizing the number of concurrent transmissions. Transmitted-Reference MAC (TR-MAC) [15], [16] is such protocol that has been designed as a possible suiter for TR (and N-FOM) communication.

However, TR-MAC has so far only been tested with mere abstractions of a physical layer. A simulation model of TR-MAC with the implementation of an N-FOM

physical layer model resulting from real modelled physical layer phenomena has to be developed. This in order to evaluate the impact of N-FOM on TR-MAC as a dedicated MAC protocol in order to see if the conclusions made in [16] still hold.

1.2 Framework

This report is written for the WALNUT project as main topic of a combined master's thesis in Computer Science and Electrical Engineering at the University of Twente. The aim of the WALNUT project is to develop new techniques for establishing robust radio links in WSNs that operate in an extremely crowded radio spectrum, at very low power, using noise-based frequency-offset TR modulation. The research encompasses multiple topics, e.g. the N-FOM and TR-MAC schemes, currently researched and designed by PhD students within the Telecommunication Engineering (TE) and Design and Analysis of Communication Systems (DACS) research groups respectively. Additionally, a PhD student within the interated circuit design (ICD) group has been working on an implementation design of N-FOM on an integrated circuit (IC), but that topic is not covered as it did not fit within the scope of this thesis.

1.3 Goal of the assignment

The goal of this thesis is to investigate the behavior of TR-MAC with the N-FOM physical layer by simulating the full N-FOM system by means of a combined MAC and physical-layer model. Here the limitations of the physical layer are not given by hard limits on the number of simultaneous transmissions, but are resulting from real modelled physical layer phenomena. The result of this research should answer the following research question:

Does the full simulation model of TR-MAC and N-FOM show any effects in TR-MAC that were previously unaccounted for, which affect the performance of N-FOM as communication method for multiple-access wireless sensor networks?

1.4 Report organization

In this report, first an intoduction is given on the N-FOM physical layer in Chapter 2. A detailed description is given on the N-FOM modularion scheme, self-correlation, multiple access, and offset criteria. Furthemore, limitations imposed by this layer are

discussed. In Chapter 3, TR-MAC, the resulting MAC protocol designed to specifically cope with the N-FOM physical layer limitations, is described as well as the effects of MA. Additionally, simulation results on the effects of N-FOM on TR-MAC are discussed and shortcomings of the current TR-MAC simulation are evaluated. Chapter 4 describes the design requirements of a joint simulation model incorporating TR-MAC as well as N-FOM, and provides a description of the full N-FOM physical layer functionality implementation. Results of the joint simulation model are evaluated in Chapter 5, verifying physical layer functionality, peer-to-peer model testing for defining the windows of interest and MA modelling. Finally, Chapter 6 consists of a conclusion answering the research question as defined in Section 1.3 and recommendations for future tests or implementations.

Chapter 2

Noise-based frequency-offset modulation

As discussed in Chapter 1, N-FOM was suggested as a more energy-efficient, and a relatively easier to implement, solution for SS communication in WSNs. However, some other limitations come with it. In this chapter a full description of N-FOM will be given to give more insight in the design criteria, its behavior and the formulas that describe it. This in order to properly model it for simulation. First, in Section 2.1, the modulation scheme is described in peer-to-peer communication, where only one transmitter is actively communicating to a receiver within a timeframe, i.e. there are no concurrent active links present. This section includes the workings of the self-correlating receiver scheme, and how frequency offsets play a role. The description of N-FOM is then extended with respect to MA communications in Section 2.2, where more insight is given in the additional design criteria for, and limitations induced by, concurrent transmissions.

2.1 Modulation

In order to determine N-FOM physical-layer effectiveness, extensive research on N-FOM modulation and transmission schemes has been performed by Bilal *et al.* [14], [17]–[19]. The N-FOM communication scheme shown in Figure 2.1 depicts a single-link communication. Within this scheme the spreading signal, i.e. band-limited noise, is sent along with a frequency-shifted version of the spread information signal and demodulated at the receiver by means of a known unique feature, i.e. frequency offset. The receiver thus does not need to know the spreading signal used at the transmitter, but simply demodulates the received signal through self-correlation. This significantly simplifies receiver design as the spreading signal is no longer generated in the receiver for demodulation, omitting the requirement of complex receiver struc-

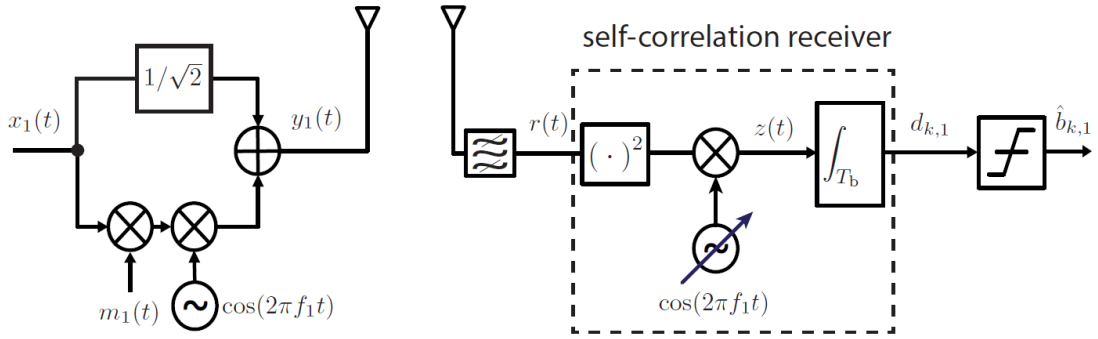

Figure 2.1: N-FOM system: Modulation scheme showing a transmitter communicating to a receiver using an unique reference. *Adapted from:* [17].

tures, e.g. rake receivers, to cope with multipath effects. The whole communication scheme works as follows. At the transmitter (or user) a narrowband message signal $m_1(t)$ is spread by the spreading signal $x_1(t)$. This signal is then shifted by using a frequency offset (f_1) much smaller than the spreading signal bandwidth (B_{ss}) [17] and is combined with the unmodulated reference signal. This modulated signal has the form

$$y_1(t) = x_1(t)\left(m_1(t)\cos(2\pi f_1 t) + \frac{1}{\sqrt{2}}\right), \tag{2.1}$$

where the $1/\sqrt{2}$ scaling factor is chosen to make sure the information signal and spreading signal have the same mean power in $y_1(t)$. Here the frequency offset f_1 is known to the receiver. A visual representation of the modulation and demodulaton process is given in Figure 2.2.

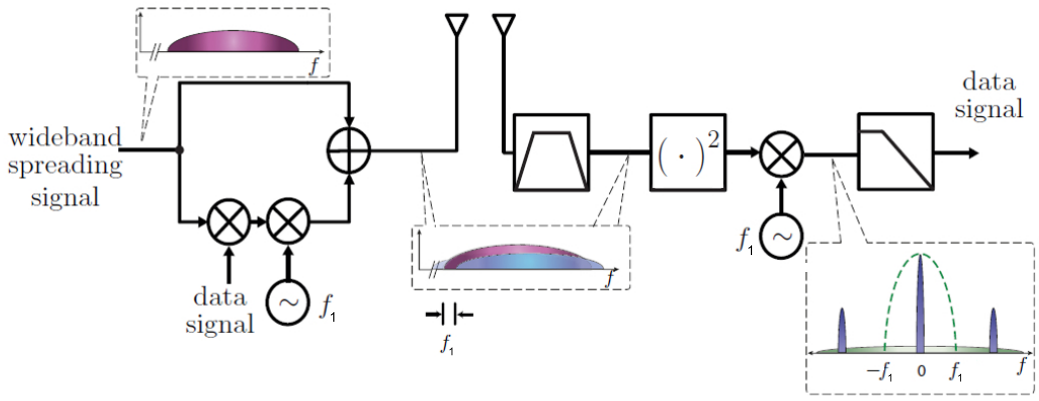

Figure 2.2: Visual representation of signals during modulation and demodulation in the N-FOM physical layer.

As can be seen the spreading signal and the data signal have significant overlap. This is due to the fact that $f_1 \ll B_x$, which will be explained in Section 2.2.1. The N-FOM communication channel is initially modeled as an AWGN channel [20], [17] as a simplified representation of reality. It should be noted that this decision has been made as first-step approach to understand the workings of the N-FOM system, but that this system is actually built for a multipath environment and needs to be extended in the future. The receiver listens to the channel and receives all data, thus also noise and unwanted transmissions, transmitted over it. The received signal is then passed through a bandpass filter to (ideally) filter out all out-of-band noise. After filtering, the message of the user is retrieved by correlating the received signal $r(t)$ with a frequency-shifted version of itself, i.e., by selecting User 1's frequency offset ($f_1 = f_r$) where f_r is the frequency offset at the receiver. This is achieved by squaring the received signal and applying a frequency offset by means of a local oscillator (LO) [17]. Although this might not be directly obvious from the receiver scheme depicted in Figure 2.1, when looking at Figure 2.3(a) and 2.3(b), it can be seen that first squaring a signal and then shifting in frequency equals multiplying that signal with a frequency-shifted version of itself. The reason for this is that the multiplication operation is commutative and the order in which the two consecutive operations are performed is irrelevant. The demodulated signal is then filtered using an integrate-and-dump filter (IDF). Ergo, Receiver 1 receives the bits of the Transmitting User 1 using f_1 and any other signals present at time of reception are filtered out or considered as noise.

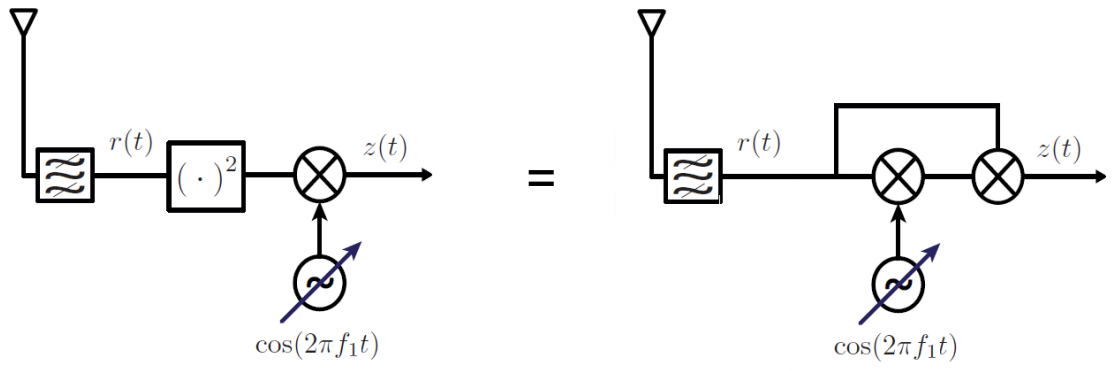

(a) Signal $r(t)$ is first squared and then shifted by a frequency offset

(b) Signal $r(t)$ is frequency shifted and then multiplied with an unshifted version of itself

Figure 2.3: N-FOM squaring and shifting operation representations.

The performance model of peer-to-peer N-FOM is given by the BER

$$\mathrm{BER} = Q\left(\sqrt{\mathrm{SNR}}\right), \tag{2.2}$$

Here $Q(x)$ is the Gaussian tail probability function,

$$Q(x) = \frac{1}{\sqrt{2\pi}} \int_x^\infty \exp\left(-\frac{u^2}{2}\right) \mathrm{d}u. \tag{2.3}$$

It can be seen that the BER results from the SNR of the decision sample

$$\mathrm{SNR} = \frac{8\gamma^2}{(25\gamma^2)\,\frac{1}{S} + 20\gamma + 8S}, \tag{2.4}$$

where $\gamma = E_\mathrm{b}/N_0$ is the received SNR per bit of the specific node. E_b is defined as the average received bit energy of the user and N_0 is the single-sided noise PSD [17]. Furthermore, $S = B_x T_\mathrm{s}$ is the spreading factor, where T_s is the symbol duration. From this model it can be seen that if the SNR per bit (γ) is sufficiently large, (2.4) will reduce to the asymptote of $\mathrm{SNR}_l = 8S/25$. Here the SNR is not longer dependent on the signal performance, but on the bitrate and the in-band noise.

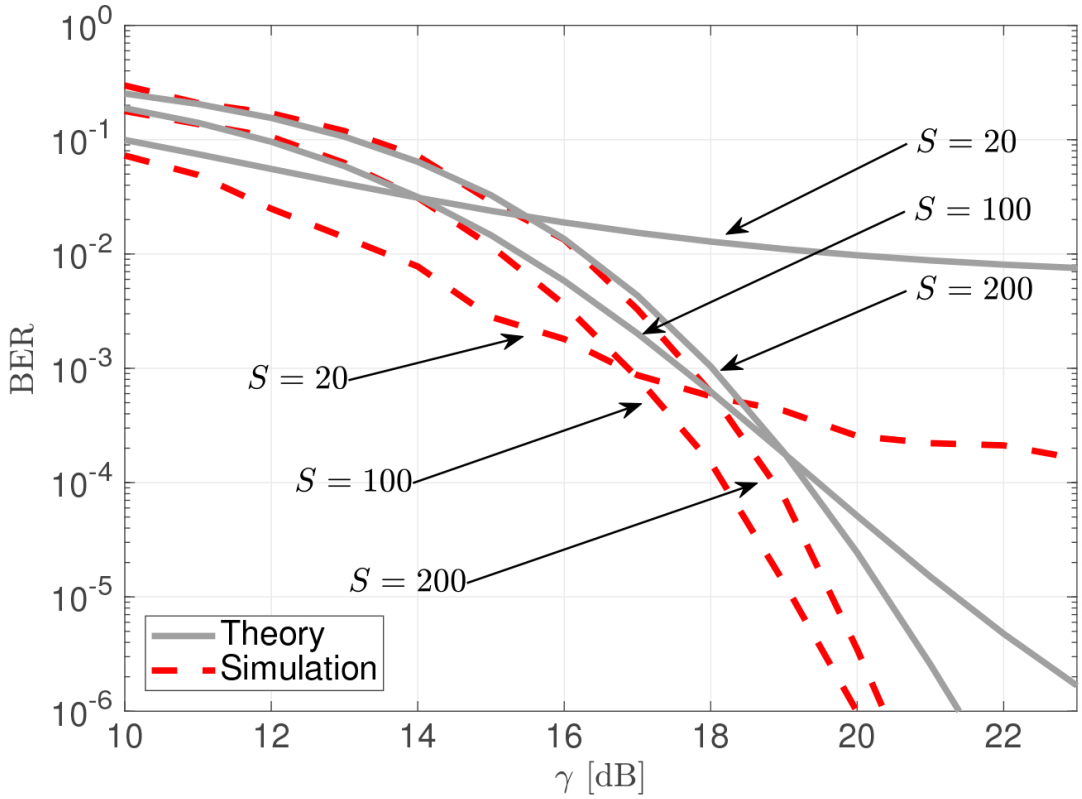

Figure 2.4: Comparison of BER between theory and simulation, for various spreading factors. *As taken from:* [21].

For peer-to-peer communication, one can plot the BER with respect to the SNR per bit for different values of the spreading factor, as is depticed in Figure 2.4. If one would like an optimal performance – rule of thumb is a BER of 10^{-3} – for which γ

is not too high, to prevent too much deviation from theoretical results, the optimal spreading factor is considered to be approximately 100 [17]. It is also apparent from Figure 2.4, that for different speading factors a different optimal γ should be selected to reach a BER of 10^{-3}. If the SNR per bit is small, however, in-band noise will take the overhand, of which the amount of noise depends on the spreading factor.

2.2 Multiplexing

As multiple wireless sensor devices often communicate in WSNs, MA is regarded as an important aspect of WSN communication. With N-FOM having MA is easily achievable by simply adjusting the frequency offset used in a specific transmitter for different communication links, as shown in Figure 2.5. Here Receiver 1 receives data from Transmitting User 1, using frequency offset f_1, and Receiver 2 received data from Transmitting User 2, using frequency offset f_2.

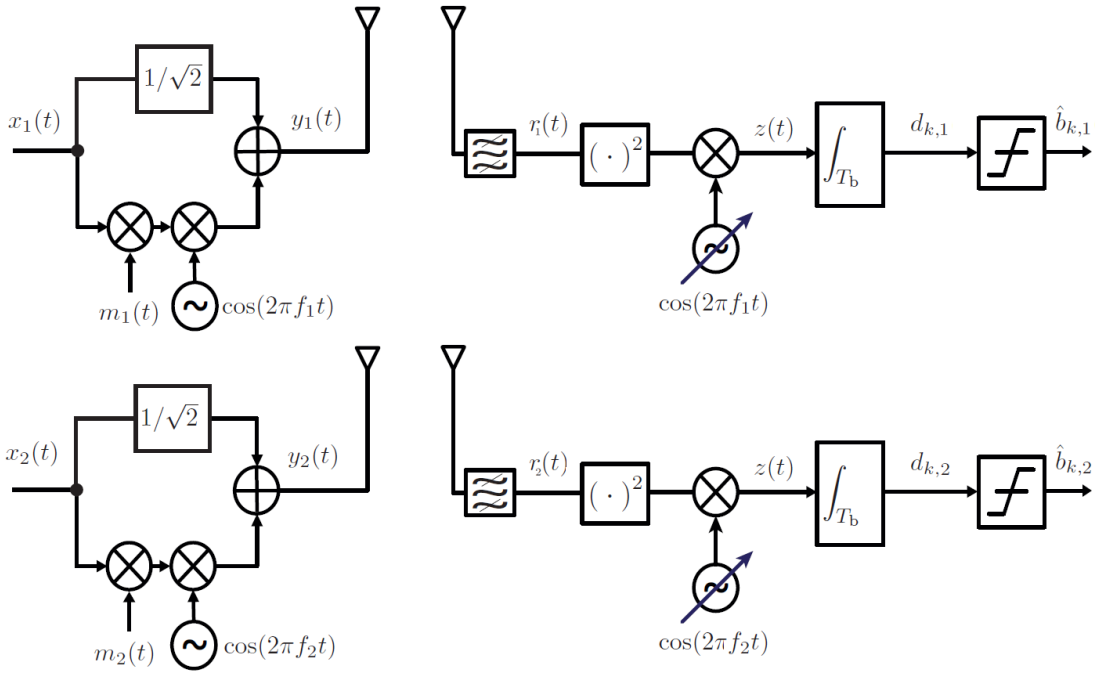

Figure 2.5: MA N-FOM system: Modulation scheme showing two transmitters communicating to two receivers. *Adapted from:* [17].

In standard MA SS communication schemes, the interference level for a specific user is primarily raised by signals from other communicating nodes. However, in N-FOM this is inherently different due to the square operator in the self-correlation block. The squaring results in the creation of additional self-mixing and cross-mixing terms between received signals and channel noise, leading to a different behavior of the noise contribution to the system [17]. Given that only the signal $y_l(t)$, where l is

the node of interest, is desired, self-mixing terms from other transmitters and noise products and cross-mixing terms between these and the signal of interest add to the overall contributed noise of the received signal. This results in a roughly quadratic decrease of the SNR in relation to number of users when the SNR per bit of the users are in the same order of magnitude. It can thus be observed that the squarer is the culprit of increasing the amount of noise at the receiver. However, this squaring operation is much needed for despreading the signal at the receiver, simplifying the dereferencing of the transmitted signal [22]. In the example of Figure 2.1, the number of noise products is still limited in number as only a single transmission occurs. However, when having a multitude of simultaneous transmitters present, e.g. Figure 2.5, the number of mixing terms in $z(t)$ increases roughly quadratically; thereby also increasing noise. The overall N-FOM performance model is given by

$$\mathrm{SNR}_l = \frac{8\gamma_l^2}{\left(25\gamma_l^2 + 17\sum\limits_{\substack{i=1\\i\neq l}}^{N}\gamma_i^2 + 20\gamma_l\sum\limits_{\substack{i=1\\i\neq l}}^{N}\gamma_i + 16\sum\limits_{\substack{i=1\\i\neq l}}^{N-1}\sum\limits_{\substack{j=i+1\\j\neq l}}^{N}\gamma_i\gamma_j\right)\frac{1}{S} + \left(20\gamma_l + 16\sum\limits_{\substack{i=1\\i\neq l}}^{N}\gamma_i\right) + 8S}, \quad (2.5)$$

where it is noticeable that the physical-layer behavior depends on the number of nodes in concurrent transmission, which is apparent due to the number of terms in the denominator [17]. In the case of one, two and three concurrent active links, the noise contribution increases significantly. These terms should be taken into account when modeling the physical layer in order for N-FOM to function according to Figure 2.1.

2.2.1 Offset criteria

In order for N-FOM to successfully distinguish between the reference signal and the modulated information signal, a frequency offset f_i is used. This frequency offset can be obtained by mixing one of the signals using a low-frequency LO [13]. For proper de-spreading of the signal, f_i at the receiver should be chosen identical to the offset selected at the transmitter. In order to distinguish between different transmitters using different frequency offsets, f_i can be varied at the receiver end by tuning the LO, allowing for MA. However, research performed by Shang *et al.* has shown that the value of f_i at the transmitter is not arbitrary [13], [23]. When choosing a value for f_i for each transmitter, one important criterion is that the selected offsets do not cause direct interference between transmitters. Therefore it should hold that $|f_i - f_j| \gg 1/T_\mathrm{b}$ and $|f_i - 2f_j| \gg 1/T_\mathrm{b}$, where $i \neq j$, and T_b is one symbol duration of the data signal [23]. This ensures that data from other transmitters with a frequency offset different to the one used in the receiver are filtered out as they fall out of band at the IDF. Furthermore, for the desired signal the frequency offset used should be significantly smaller than the spreading signal bandwith. This is to assure that the reference and information signal are significantly overlapping and

not distorted by the band-pass filter at the receiver [14], [18]. Additionally, in MA, a spreading factors larger than 100, i.e. the optimum spreading factor in single node communication, is desired for better SNR per bit at the receiver.

2.2.2 Near-far effect

In Shang's research the assumption was made that the signals from different users are received at the receiver with equal strengths, which is not realistic. In practice, due to the disparity in distances between transmitters, the signal from each transmitter experiences a different amount of attenuation. The difference between these signal strengths could lead to the near-far effect at the receiver end [17].

Generally speaking, the near-far effect (or near-far problem) occurs when the received signal power of one transmitter is significantly higher than the power received from another transmitter, resulting in complete jamming of the signal from faraway transmitters [24], [25]. Thus, for example, when looking at Figure 2.6, in the case of receiver R_1, the receiver is close to transmitter T_1. Here the received power of T_1 is significantly larger than the received power of T_2, making it difficult (or impossible) to detect both signals and possibly jamming the weakest transmitter. This is also known as the near-problem. In case of receiver R_3, transmitter T_1 is too far away, resulting in the fact that T_1 is too weak to be tracked by the receiver. This is called the far-problem. However, in the case of receiver R_2, where the receiver remains between the near- and far boundaries, the receiver is in the so-called effective dynamic range (EDR) zone. Here both transmitters can be tracked by the receiver. The EDR is defined as the ratio between the strongest and weakest signal where the receiver can still demodulate the signals without excessive noise or distortion [24].

In research performed by Bitachon *et al.*, it has been observed that the MA interference has a significant impact on the basic N-FOM system [17]. Results have shown that the near-far problem imposes critical limitations on the N-FOM system. Here the presence of a strong user severly degradates the BER of a particular user of interest when both are transmitting simultaneously [17]. This is primarily due to the self-correlating nature of the receiver (see Section 2.1), where the decrease in performance is primarily attributed to the interference self-mixing product. Theoretically the limitation invoked by these self-mixing products introduced during demodulation result in unacceptable BERs for more than three concurrent active links [17].

2.2.3 In-band interferences

In-band interferences induced by other systems also pose a significant threat, as these interferences can significantly impact the performance of N-FOM [14], [20].

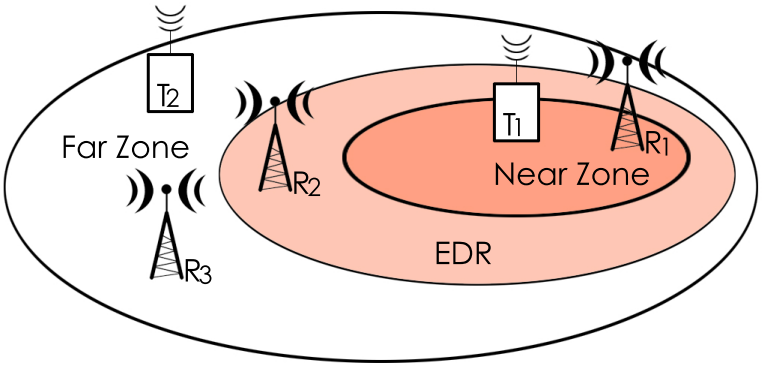

Figure 2.6: Example situation with near-far regions

For smaller bandwidths of the in-band interference, however, the signal distortion caused by the dominating term can be reduced if a frequency offset is selected that is significantly larger than the interference bandwidth [14].

2.3 Conclusion

Within this chapter a detailed literature review on N-FOM has been given. A description has been made for the N-FOM physical layer in single-link communication to explain the main features of the modulation and demodulation schemes which has then been extended to performance in MA. Additional requirements for MA communication have been explained and the impact of multiple concurrent active links have been described. Based on the results and conclusions of Bilal's and Bitachon's research, the strengths and weaknesses of N-FOM have been summarized.

In general, N-FOM physical layer looks promising as physical layer for use in WSNs due to its fast synchronization and low-power capabilities. However, in order to prevent severe deration in the BER, further research in noise reduction would be required along with the implementation of a MAC protocol. This in order to solve the physical layer limitations and to obtain a higher efficiency in MA communication and will be discussed in Chapter 3.

Chapter 3

Transmitted reference medium access control

As apparent from Chapter 2, the number of possible concurrent active links is severely limited as a result of the self-mixing products generated in the demodulation scheme. Invoking a restriction on the maximum number of concurrent active links allows for better BER at the receiver with proper demodulation of the desired signals. In MA wireless communication the MAC protocol is the key element in performing medium access control for the medium shared among transmitters. In general the MAC protocol regulates the network by providing addressing and channel access control mechanisms, allowing nodes to communicate within an MA network. Given that the number of concurrent transmissions has to be regulated for a proper BER at reception, the use of a MAC-protocol is a necessity. However, as TR (and thus also N-FOM) is designed such that the receiver receives a reference along with the information signal, as opposed to coherent receivers, additional power consumption during transmission is imminent as additional signals are sent. Energy efficiency is considered an important requirement in the design of communication protocols for WSNs due to limited power [26]. Besides regulating the network in MA, the MAC layer itself has the important task to fine-tune and adapt the duty cycle of the transmitter and receiver in such a way that low-duty cycle communication is achievable; i.e. in order to enhance the lifetime of WSN nodes, the MAC layer should ascertain that both transmitter and receiver sleep most of the time and spend the least amount possible time to transmit, receive and listen to the channel. The MAC layer could thus exert a large amount of influence on the energy consumption, and therefore be of assistance in lowering the power consumption of N-FOM. This led to more research on a suitable energy-efficient MAC protocol, giving birth to TR-MAC.

Within this chapter, a description will be given of the design of TR-MAC and how it copes with the mechanics of the N-FOM physical layer. A description will be given on the types of communication states that occur using the TR-MAC protocol in N-FOM

communication in Section 3.1. Additionally, another model will be introduced in order to provide a better understanding on the limitations imposed by concurrent active links in N-FOM for the TR-MAC layer and how a multi-channel approach can aid in solving this issue in Section 3.2. Finally, based on the outcomes of this additional model, a full description of TR-MAC in MA will be given in Section 3.3.

3.1 TR-MAC

The main motivation for the design of TR-MAC was to exploit all the advantages of N-FOM [15], [26]–[28]. The TR-MAC protocol consists of three states, as depicted in Figure 3.1; these states are (1) first-time communication, (2) unsynchronized link, and (3) synchronized link [15].

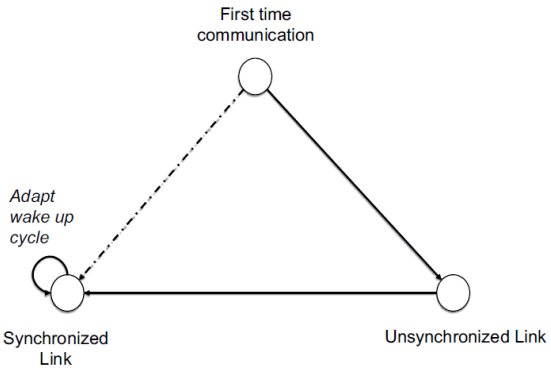

Figure 3.1: TR-MAC communication states. *As adapted from:* [15].

A visual representation of the unsynchronized and synchronized state is shown in Figure 3.2 and works as follows. In the unsynchronized link and first-time communication state, Figure 3.2(a), a node does not have any information of its neighbors. In order to set up a synchronized link with a specific receiver, the node has to let know it is present by sending a preamble with a predetermined frequency offset which receivers listen to when they are not in synchronized communication and are not sleeping. For this purpose TR-MAC does not use preamble sampling, where normally a transmitter would transmit a very long preamble, with length of at least one duty cycle, to make sure the receiver wakes up and is informed that it should stay awake to receive an upcoming data packet. Instead, TR-MAC repetitively sends short preambles along with the data packet. A receiver that wakes up and receives the short preamble will reply with an acknowledgement (ACK) if it is listening to the unsynchronized link frequency, or goes back to sleep respectively. The transmitter listens to the receiver's ACK and halts its transmission, whereas normally the long preamble still had to be finished, allowing for swifter transmissions

and shorter wake-up periods in the receivers. Subsequent to preamble reception, neighbor discovery is performed, MAC addresses are exchanged, and a link identifier is determined. After initial communications, the protocol is in unsynchronized transmission. In this stage the transmitter transmits small data bursts to the receiver. If the receiver detects a packet, the transmitter is identified based on the link identifier assigned. Based on this packet, receiver wake-up times are agreed upon by both ends and a unique frequency offset is allocated for communication. This allows for both receiver-driven or transmitter-driven communication. As a result, the nodes are in the synchronization stage of the protocol.

Synchronized communication is depicted in Figure 3.2(b). In this communication state, the transmitter wakes up in the agreed-upon timeslot to transmit his data along with a short preamble containing a specific frequency offset meant for a specific receiver. A receiver that wakes up and receives the short preamble directly knows whether or not the preamble is meant for it and will send out an ACK or goes back to sleep respectively. This allows for the transmitter and receiver to keep transmission to a minimum [15]. Additionaly, duty cycle adaption can be performed in order to cope with event-driven situations, to maintain energy efficiency. This makes TR-MAC a suitable MAC protocol for low-data-rate applications, e.g. WSNs.

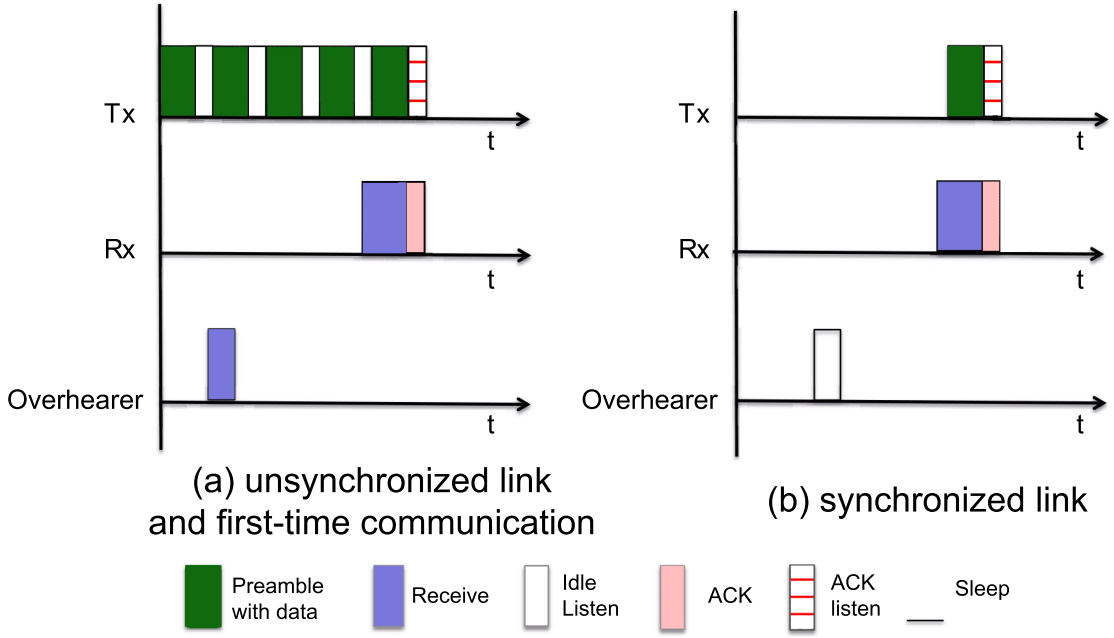

Figure 3.2: TR-MAC unsynchronized and synchronized protocol. *As adapted from:* [15].

The downside of TR-MAC, as defined in [15], [26]–[28], is that, in a highly dynamic situation, TR-MAC might not perform that well, as it was originally designed for low data rate WSNs [27]. Morshed therefore suggested to extend TR-MAC with

traffic-adaptive duty cycling and request based burst packet transfer in order to cope with increasing traffic load [16], [27]. Furthermore, multiple-link scenarios and the limitations imposed by N-FOM, e.g. the near-far effect and mixing noise products, have not been considered here.

3.2 Slotted Aloha model

In order to gain a deeper understanding of the multi-channel properties and the TR limitations imposed by N-FOM, Morshed *et al.* proposed a MAC-layer model abstraction in [29] for the main purpose of providing an insight on the fundamental limitations of TR (and N-FOM) at MAC level.

For this model, single-channel Slotted Aloha (S-Aloha) was selected as a starting point [30]. Morshed *et al.* extended this model to a multi-channel S-Aloha version. The model uses multiple frequency offsets implemented as seperate channels with each channel. A node can randomly and independently choose any of the channels for a time slot to transmit a packet [29]. Additionally, the model only allows for a maximum number of simultaneous transmitters, based on the system characteristics of N-FOM [17] for a successful communication.

Additionally, Morshed concluded that a larger number of available frequency offsets yield a better thoughput in the system and thus a better efficiency with a limitation on the number simultaneous communications. Efficiency decreased when the maximum number of simultaneous communications was increased. Morshed thus found that a frequency offset based system performs best if the pool of available offsets to choose from is significantly larger than the number of allowed concurrent simultaneous transmissions. [29] and is discussed in Section 3.3. The results gathered from the multi-channel S-Aloha model provided fundamental and deeper insight into the design criterion of a MAC protocol that exploits TR modulation.

3.3 TR-MAC in multiple access

Based on the findings in Section 3.2, Morshed has been looking at the consequences of using TR modulation as physical layer in combination with TR-MAC from an MA perspective [16]. Although TR has the inherent possibility for MA communication by using different frequency offsets, it it still desired to prevent that multiple transmitters utilize the same frequency offset at the same time. Additionally, it should be prevented that too many transmitters transmit simultaneously to maintain efficiency as discussed in Section 3.2 and to keep noise contribution due to mixing products of other transmitters to a minimum as explained in Section 2.2. To prevent

this, Morshed concluded mechanisms are required that prevent simultaneous use of frequency offsets and limits the number of concurrent active links. Frequency allocation management thus had to be implemented.

Morshed concluded based on his research [16] that the available number of frequency offsets is limited to 26, due to the fact that the maximum number of frequency offsets selected has to be much smaller than the coherence bandwidth to make sure signal and reference are affected equally by the propagation channel. This value represents the number of usable frequency offsets from a limited pool of 40 available offsets in an indoor office environment [16], which was determined by dividing the maximum value useable as frequency offset (approximately a tenth of the coherence bandwidth), by the bitrate of 25 kbps. This number is limited in order to ascertain reference and message signal are still in the same propagation channel. From these offsets, one is reserved for unsynchronized transmission; hence, every node can form a maximum of 25 transmission pairs in their synchronized link state. Furthermore, the maximum available check interval duration across the network is divided by the maximum number of available frequency offsets, i.e., 25 time instances are allocated for node check intervals, each bound to a unique frequency offset. Results gathered from this model abstraction provided deeper insight into the design criterion of a MAC protocol that exploits TR modulation.

Additionally, in order to prevent unnecessary contention as a result of cross-mixing products, TR-MAC is designed in such a way that every frequency offset is uniquely allocated to a transmitter by a receiver upon synchronization and is attributed to a non-overlapping transmission opportunity, transmitters paired to the same receiver in synchronized state will never show concurrent transmissions; basically behaving like peer-to-peer communication. As Morshed allocated a total of 25 unique frequency offsets for synchronization, each receiver can be maximally paired to 25 transmitters which are then attributed each their non-overlapping transmission opportunity related to the offset used. In the case of MA in sparse networks, where a low number of nodes are distributed over a significantly large area and not all nodes will be able to see each other, this would most likely mean that no overlap in transmissions is present between different transmitter-receiver pairs communicating as nodes are not synchronized with each other outside their pairs and wake up at random time intervals. In other words, the probability that in a sparse network random nodes wake up in approximately the same timeslot out of all timeslots available is extremely small, resulting in a high probability of communication without concurrent active links present. Additionally nodes perform channel sensing prior to transmission, resulting that a random back-off time is scheduled if the channel is sensed to be busy [16].

In the case of very dense MA networks, where an area is saturated with nodes, however, the probability of concurrent transmissions increases significantly, resulting in more mixing products contributing to more noise in the receiver, decreasing throuhput and lowering the system's efficiency. Due to the incorporation of channel sensing, however, this can be prevented by adding random backoff delays to nodes if the channel is sensed busy; or forcing the nodes back into unsynchronized state if too many backoff attempts have been performed and no other frequency offsets are available. Peer-to-peer communication is thus still performed to a large extent. However, as the number of active links in the network increases the probability on having more concurrent active links increases as well. This is also depicted in Figure 3.3. Here Morshed plotted the thoughput against the number of active links present. As can be seen if the environment is heavily saturated by nodes, and therefore a resulting larger number of active links, the throughput collapses as too many concurrent active links are present, resulting in too much interference at the receiver causing all concurrent communications to fail.

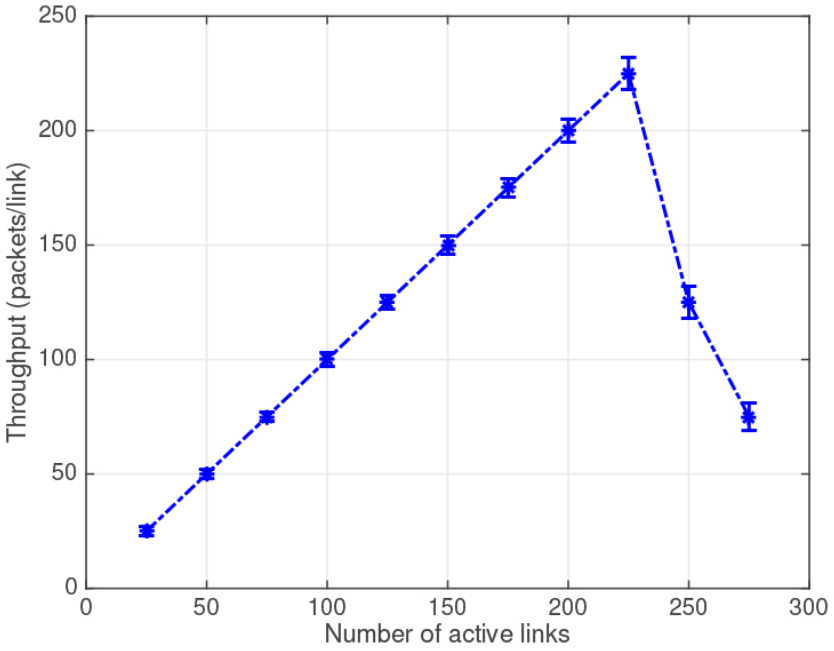

Figure 3.3: Throughput performance for varying number of active links. *As taken from:* [16].

An additional issue that arises is that hidden terminals are bound to occur, where transmitting nodes sensing the channels are too far away from each other to sense the channel is busy, but the receiving nodes are close enough to cause inteference on each other. If this includes too many concurrent active links, collisions might occur. Therefore, proper collision management has to be implemented. From a

protocol point of view collisions are costly. Energy is consumed by receiver and transmitter without having succesful communication, requiring retransmissions with the result that the receiver has to be awake again for reception in the future. As discussed in Sections 2.1 and 3.2, the system performance severely decreases if the number of simultaneous transmissions increases due to the unwanted mixing products. This could result in dropped packets. In other words, TR-MAC thus has to manage retransmission techniques. For the case of the unsynchronized link, transmissions intervals are utilized to determine problems of communication. If no ACK has been received within the maximum interval duration, a problem is concluded, and retransmission has to be performed. If transmissions continue to fail for a number of retransmissions, the receiver node is considered dead or out of range [16]. For synchronized transmissions, a missed ACK would mean an out-of-sync scenario. In order to regain synchronization, the MAC protocol has to ensure that the nodes in a synchronized pair update their transmission times or change their frequency offsets to prevent further collisions. The downside of this, however, is that the synchronizations are discarded too quickly if no ACK has been received. Another solution proposed is falling back to the unsynchronized state, and attempting to regain synchronization. This has the drawback that contention increases [16].

3.4 Conclusion

Within this chapter a detailed literature review on TR-MAC has been given. A description has been made of the link states of TR-MAC and how unsynchronized and synchronized link transmissions function. Additionally, it is explained how TR-MAC uses small data bursts for first-time communication instead of a preamble sampling mechanism for shorter communication times. Furthermore, an extension of TR-MAC has been given for use in MA where it exploits the TR feature of the N-FOM physical layer. Based on the results and conclusions of Morshed's research, the strengths and weaknesses of TR-MAC have been summarized.

In general, TR-MAC has been proven effective for use in MA communication utilizing frequency offsets and looks promising MAC implementation for the N-FOM physical layer. However, Morshed did not take physical layer phenomena into account as the focus of Morshed's research was primarily on modeling the phenomena on a MAC level in terms of communication states and (possible) concurrent transmissions. As a result, Morshed used an abstraction of the physical layer. Besides taking care of the design of proper communication states, the effects imposed on the MAC by the physical layer also have to be taken account. To test the performance of the physical layer in conjuction with TR-MAC a simulation model is required. The design of such simulation model is discussed in Chapter 4.

Chapter 4

Simulation model design

In order to test the functionality of TR-MAC, Morshed created a simulation model [16]. This simulation model has been built using the OMNeT++ [31] discrete event simulator extended with the (currently deprecated) MiXiM [32] mixed simulator package, allowing for easier and more user-friendly MAC integration. Within this simulation Morshed implemented an abstracted version of the N-FOM physical layer characteristics as investigated by Bilal *et al.* [14], [17]–[19]. However, no mixing effects or cross-correlation effects have been included. The transmission power has been mapped together with the carrier frequency to transmit a signal over the transmission channel modelled in the TR-MAC simulation model. The channel has been characterized by Friis's free-space path loss model, attenuating the transmitted signal based on distance and carrier frequency, but omitting any fading phenomena such as shadowing and scattering effects. If the received power is larger than the receiver sensitivity, the transmission is deemed successful. Channel noise and interferences have thus not been taken into account [16] and a hard limit was set on the number of simultaneous transmissions. A block implementation of the MAC and physical layer in MiXiM can be seen in Figure 4.1.

In Figure 4.1 it can be seen that the TR-MAC layer is an extension of the base MAC layer of MiXiM, handling all the basic functionality of a MAC layer, e.g. upper and lower level message handling, battery access etc. This allows for modularity in the sense that different MAC layers can be applied without requiring to change a significant amount to the simulator. A similar approach applies to the base physical layer. Both these layers communicate to each other through the base layer in which MiXiM handle MAC-physical layer and physical layer-MAC interaction. The MiXiM Core contains all the functions and files required to make the mixed simulator package run in OMNeT++. It can be seen in Figure 4.1 that Morshed extended the base physical layer with an SNR threshold decider. Within this decider block, the SNR of a signal during transmission is compared to a certain threshold. If the signal is above the threshold at all times during transmission, the communication

is deemed successful – else the packet transmission fails due to “interference” and “packet corruption”.

Simulations performed have given insight that receivers are able to synchronize with multiple transmitters allowing for better throughput. However, when the number of transmitters increases the thoughput descreases significantly, imposing a limitation on the number of concurrent receiver-transmitter pairs [17]. Although Morshed *et al.* have proven that multi-channel TR communication using TR-MAC is functional and successful, the physical layer is based solely on abstractions directly implemented in the MAC-layer. The MAC layer has not yet been simulated with a proper physical-layer implementation. A more realistic physical-layer model has to be implemented to test the model’s overall effectiveness.

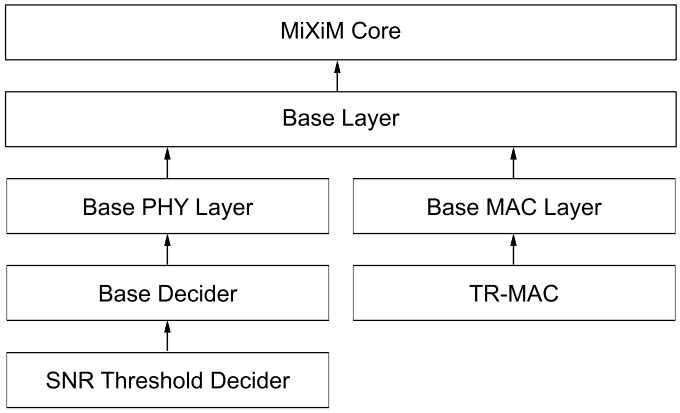

Figure 4.1: Simulation model block diagram of MAC and abstracted physical layer implementation in MiXiM

To test TR-MAC together with the N-FOM physical layer, an integrated testing model thus had to be made. For this purpose, Bilal’s physical-layer design, discussed in Chapter 2, was combined with Morshed’s TR-MAC model explained in Chapter 3. As a starting point, Morshed’s MA TR-MAC simulation model was used. The motivation to extend Morshed’s model whilst building upon deprecated software is twofold: first, the goal of this master’s thesis is to test the efficiency of the current TR-MAC model design in conjunction with a properly modelled N-FOM physical layer, not to rebuild the MAC-layer on its own; and secondly, rebuilding the TR-MAC model would take a significant amount of time, which simply does not fit within the scope of this thesis.

In this chapter, Section 4.1 gives a detailed description of the TR-MAC simulation model. This section summarizes the main design aspects and functions of TR-MAC as used in the OMNeT++ simulator. Extending on TR-MAC, Section 4.2 will then discuss the improved physical-layer model design and the inclusion of the N-FOM physical layer, stripping TR-MAC from its static hard limits.

4.1 TR-MAC model

For the design and implementation of the TR-MAC simulation model, Morshed has used a receiver-driven communication strategy in the scope of his thesis [16]. Here the receiver allocates a frequency offset to the sender node once the first successful transmission has taken place and moves to the synchronized link state as discussed in Chapter 3 (Figure 3.1). Within this model, each node utilizes an event-based data structure in order to track events on a chronological basis. Furthermore, nodes also keep track of their neighbors and their respective communication states. Nodes are allowed to communicate to each neighbor in unsynchronized state using a dedicated frequency offset, or in synchronized state with an agreed-upon offset tracked by the receiver of interest during a prior specified timeslot. The TR-MAC model uses carrier sense and has a backoff mechanism incorporated; i.e., nodes listen to the medium prior to sending packets and back off if the channel is busy. Furthermore, a retransmission mechanism is incorporated to account for packet loss and collisions.

Additionally, as discussed in [16], a maximum number of 26 frequency offsets was derived for synchronized transmission pair allocation per receiver and the overall system parameters used for this model are given in Table 4.1, but seem rather arbitrarily chosen. The transmit power, however, is selected as twice the power of other WSN MAC-protocols as there is a 3 dB loss in the transmitter due to the signal being sent twice, of which only half contains the information. This assumption, although seems logical, does not completely hold as there is an additional 7.8 dB loss in SNR due to the noise-mixing products in the self-correlation receiver in the optimal case, resulting in a total of at least 10.8 dB deficiency in comparison to other systems.

Table 4.1: TR-MAC system parameter values. *As derived from:* [16].

Preamble duration	Header duration	Data duration	ACK duration	Periodic listen duration	Tx power	Rx power	Sleep power
8 bits	16 bits	32 bits	24 bits	40 bits	2 mW	1 mW	15 µW

In order to give a better overview of the model operations, Morshed's finite state diagram [16] of the TR-MAC model for MA is given in Figure 4.2. Within this figure, node communication states are shown in conjunction with the criteria to switch from one state to another in the finite state diagram. This contains both unsynchronized communication, using a standardized frequency offset, as well as synchronized communication, where nodes communicate paired to specific receiver nodes and agreed-upon frequency offsets.

Whenever a node initializes and passes the INITIALIZATION state for the first time, the respective node goes to SLEEP and starts in the unsynchronized link state. Within this SLEEP phase the node uses predetermined wakeup times to sense the medium for activity of other nodes using the standardized frequency offset and moves to the CLEAR_CHANNEL_ASSESSMENT state. If nothing is received and the node has no packets to send, it returns to the SLEEP state and schedules a new wake-up time after a globally known check-interval duration to prevent possible channel contention. If any communication was detected during the CLEAR_CHANNEL_ASSESSMENT state, the node moves to the WAIT_DATA state until a complete preamble data packet is received. If the data is not of interest for this specific node, or if an ACK is received, the preamble is discarded and goes back to its SLEEP state. However, if the received preamble packet is destined for the node, the node moves to the SEND_ACK state to send an ACK back to the respective sender.

Within the SEND_ACK state, a node can decide to move to the synchronized link state if the transmitting node is willing to synchronize and a shift is made to the synchronized state for receiver-driven communication. Furthermore, nodes are added to a neighbor list with agreed-upon frequency offset and wake-up time for communication if they were not in there yet. Additionally, this synchronized listen event is added to the event list. In this SEND_ACK state, the current node sends an ACK back to the transmitting neighbor node and returns to its SLEEP state. Whenever this node wakes up in its next periodic wake-up periods, the node can either listen using the standardized frequency offsets for detecting or sending to unsynchronized links; or the node can wake up during an agreed time instance to receive or send a packet from or to a known synchronized neighbor pair using a predetermined frequency offset. This, however, depends on which event is scheduled first.

In the case an ACK is missed, the respective node schedules a retransmission event in the event list specifying the receiving node of interest. If there are multiple failed retransmission attempts, i.e., no ACKs received; the transmitting node will move back to the unsynchronized state and drop the packet after a maximum number of retransmissions. Additionally, a random backoff period is introduced between retransmissions in the unsynchronized state to prevent channel contention.

4.2 Physical-layer model

Originally Morshed's OMNeT++ simulation model design included a very basic physical layer abstraction, as full N-FOM physical layer implementation did not fit within the scope of his thesis. However, as TR-MAC is specifically designed to cope with the N-FOM physical layer, a fully incorperated physical layer model is much needed to test the overall behavior and efficiency of the TR-MAC protocol.

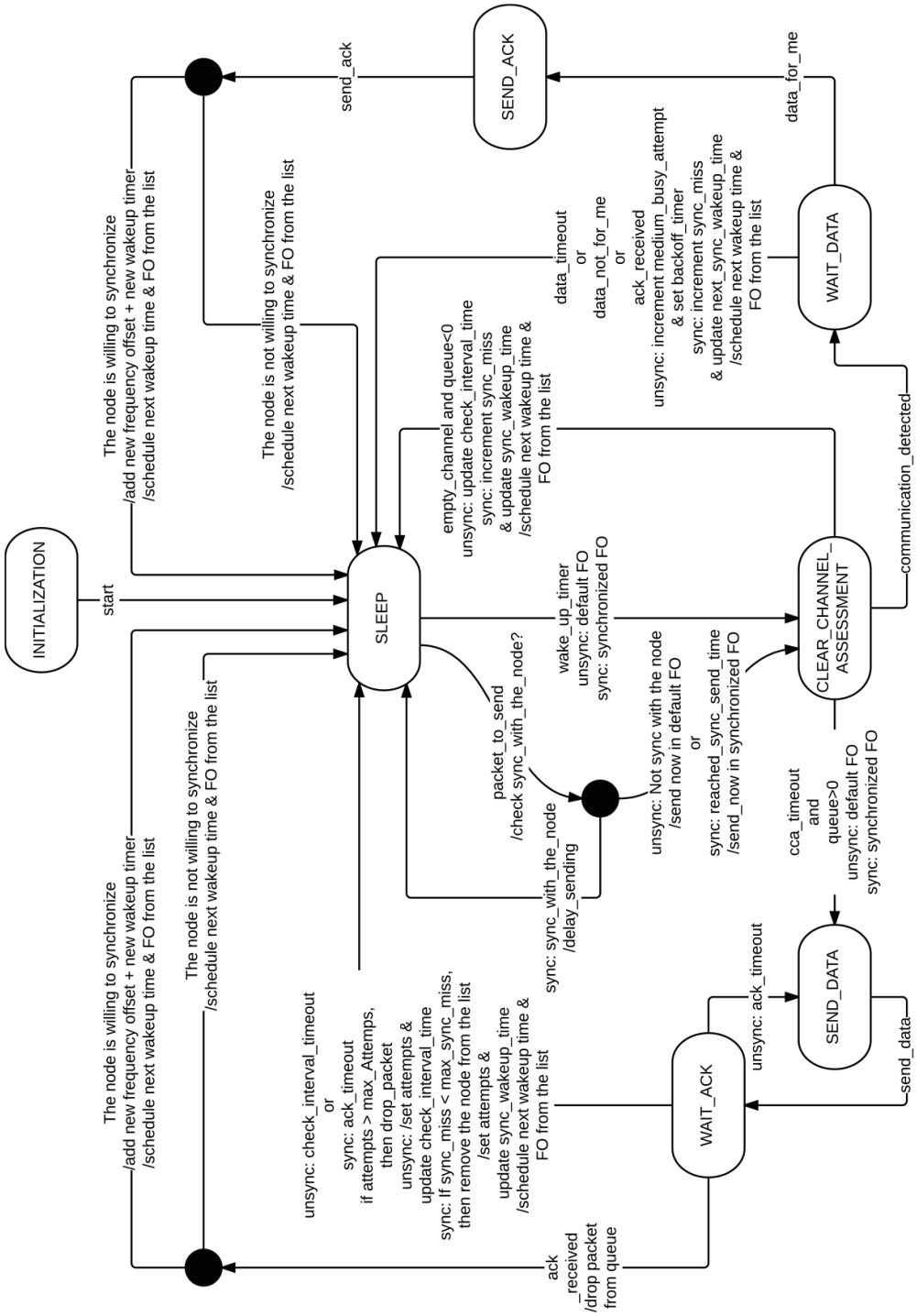

Figure 4.2: TR-MAC model operation finite state diagram. *As taken from:* [16].

4.2.1 Modulation scheme

As the goal of this thesis is to test TR-MAC efficiency and feasibility with Bilal's physical layer design, the N-FOM model is directly modelled after the modulation scheme as depicted in Figure 2.1, which was explained in Chapter 2. However,

modeling changes on bit-level where every step in the N-FOM modulation scheme that alters the signal is discribed and accounted for into OMNeT++ would require a large number of relatively complex calculations per transmission, significantly slowing down the simulator. In order to overcome this issue, Bitachon's N-FOM node SNR mathematical expression [17] that describes the BER as a function of the received SNR per bit, as explained in (2.5) in Section 2.2, has been used as a starting point to model the N-FOM modulation scheme. It should, however, be noted that the calculated node BER through the SNR at the receiver (SNR_l) is the SNR after demodulation and the IDF, and therefore should not be confused with the SNR directly at the antenna of the receiver where it is usually measured. This is advantageous for this specific use-case as the SNR_l closed-form expression completely incorporates the modulation and demodulation effects; consequently describing the N-FOM physical-layer behavior through a black-box principle. Resulting from (2.5) the BER can be calculated by (2.2) as explained in Section 2.1.

The use of (2.5) for modeling the N-FOM physical layer behavior is justifiable as Bilal *et al.* have proven that the theoretical closed-form approximation roughly follows simulations from the full N-FOM communication model for large values of the spreading factor [21]. The theoretical closed-form expression roughly follows the results from simulation down to approximately 10^{-3} BER. This is good enough for N-FOM simulation purposes as is expected that signals below 10^{-3} BER have a significantly small packet error probability; i.e. packets have a chance on packet errors in the range of 1 percent or less, with appriopriate spreading factor chosen, resulting in practically no errors after demodulation. Additionally, it should be noted that the objective of this thesis is to test TR-MAC using the N-FOM physical layer; not to verify it, as this has already been done in Bilal's research.

4.2.2 Packet error detection

In order to determine whether or not received packets have errors, Morshed compared SNR outcomes to a predetermined threshold to determine successful transmissions [16]. If the SNR of the received signal dropped below this threshold, the packet was deemed lost. Eventhough this method weighs the quality of the signal received, it is not a very reliable one. The determination of such threshold depends on a lot of factors involving the SNR and cannot be chosen arbitrarily. Furthermore, the behavior of a decider that compares the SNR to a threshold might not cope correctly if the SNR is at the boundaries of the threshold. In the case of Morshed's physical layer Morshed modeled it in such a way such that propagation effects do not influence the TR-MAC model. This in order to ascertain that only the effects of concurrent active links utilizing the same frequency and the effects of too many con-

current active links in the network are detected; the latter was modeled in the MAC layer as an abstraction. Additionally the physical layer abstraction used was a simple peer-to-peer communication model provided by the base physical layer and SNR threshold decider blocks as depicted in Figure 4.1. Here the SNR was described as the carrier-to-noise ratio (CNR):

$$\text{CNR} = \frac{P_\text{r}}{P_\text{n}} = \frac{P_\text{t}/L_\text{FSPL}}{N_0 B_\text{ss}} = \frac{P_\text{t}\left(\frac{\lambda}{4\pi d}\right)^2}{kT_\text{sys}B_\text{ss}} \tag{4.1}$$

where P_r is the received power at the antenna, P_n the in-band noise power, P_t the transmitted power, L_FSPL the free-space path loss, λ the wavelength of the transmitted signal, d the distance between transmitter and receiver, and N_0 the thermal noise PSD which is given by Boltzmann's constant k and the system temperature T_sys in Kelvin. The system temperature is descibes as

$$T_\text{sys} = T_\text{s} + T_\text{e} = T_\text{s} + (F_\text{s} - 1)T_0, \tag{4.2}$$

where T_s is the antenna temperature, T_e the equivalent temperature of the receiver, F_s the standard noise figure (NF), and T_0 room temperature. Often it is considered that $T_\text{s} = T_0$, which is practical in case the antenna sees a lot of objects in its field of view that are room tempeature (T_0). This was also considered in Morshed's abstraction, resulting in

$$T_\text{sys} = F_\text{s}T_0. \tag{4.3}$$

Evidently, it thus follows that

$$\text{CNR} = \frac{P_\text{t}\left(\frac{\lambda}{4\pi d}\right)^2}{kT_0F_\text{s}B_\text{ss}} \tag{4.4}$$

It should, however, be noted that this does not describe any cross-mixing effects due to the N-FOM self-correlation demodulation scheme.

For the case of the N-FOM physical-layer model, instead of a static threshold a stochastic process is chosen where the packet error generation is determined by a random process to model a channel that is not 100 percent reliable. In N-FOM additional noise products are generated as a result of cross-mixing. The amount of noise at the receiver highly depends on the number of concurrent active links present in the transmissions period of the node of interest. The received SNR (SNR_l) after demodulation is thus primarily determined by the active links' SNR per bit. Based on the SNR_l a BER can be calculated. The acceptence of a packet is then characterized by a transmission success process. It is assumed that this transmission success

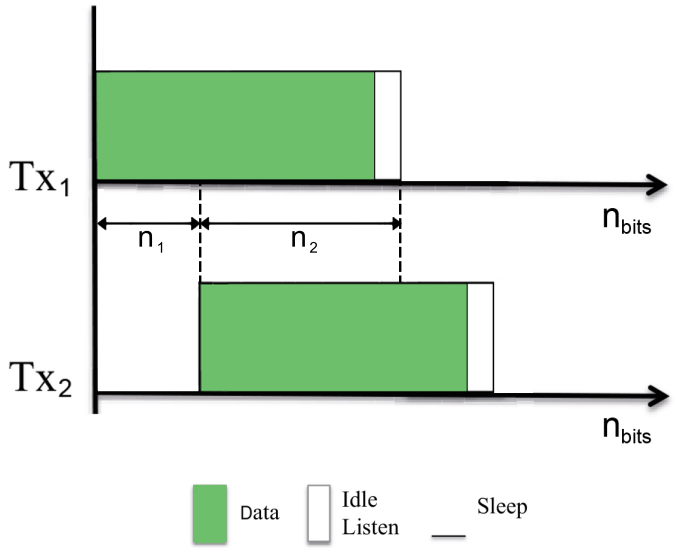

Figure 4.3: Two packet transmissions by separate transmitters with partially overlapping packets.

process is a Bernoulli process with success probability $1 - p$, where $p \in [0, 1]$ is the packet loss probability [33]. Within this process it is assumed bit errors occur independent of each other. Therefore the packet loss probability can be calculated as:

$$p = 1 - (1 - \mathrm{BER})^n, \tag{4.5}$$

where the BER is calculated using (2.2) and n is the packet length in bits. Here the packet is assumed to be lost if p is larger than a randomly selected and uniformly distributed value between 0 and 1.

It should, however, be noted that (4.5) only holds if concurrent transmissions are perfectly synchronized. In the case of not exactly overlapping transmissions for concurrent active links, the packet loss probability changes as the BER changes when more packets starts overlapping. This is shown in Figure 4.3. Here it can be seen that during packet transmissions of Tx_1 the packets are partially overlapping the transmitting packets of Tx_2. Here the first n_1 bits of packets from Tx_1 do not overlap with Tx_2, resulting in a different BER than the following n_2 bits. The correct packet loss probability function would then be

$$p = 1 - (1 - p_{b,1})^{n_1}(1 - p_{b,2})^{n_2}. \tag{4.6}$$

The overall probability is thus the combined packet error probabilities of the non-overlapping BER and the overlapping BER. This can be generalized to

$$p = 1 - \prod_{i=1}^{N} (1 - p_{b,i})^{n_i}, \tag{4.7}$$

where N is the total number of different overlaps, and thus different BER values, within a single packet transmission.

4.2.3 Channel model

In order to have a fully functioning physical layer model, the propagation channel between receiver and transmitter has to be described. For the current channel model Friis's free space path loss model has been used resulting in the following free-space path loss (FSPL):

$$L = \left(\frac{4\pi d}{\lambda} \right)^2, \tag{4.8}$$

where λ is the wavelength corresponding to the carrier frequency and d is the distance between transmitter and receiver. Effects such as shadowing and small-scale fading thus have not been included. The primary reason for this is that (2.5) also does not account for these effects. Using a fading model in combination with (2.5) would give incorrect results. This, because in (2.5) the assumption has been made that γ_l is a known value, whereas in the case of fading γ_l varies and has delay dispersion effects. These effects have not been accounted for in (2.5) as it is assumed during derivation of the equation that the received signal is a scaled representation of the transmitted signal without distorted. The main motivation for not updating (2.5) is that the scope of this thesis is to design a simulation model incorperating both N-FOM and TR-MAC from Bilal's and Morshed's research respectively. As not enough research has been performed to generate a closed-form approxation of the N-FOM physical layer that includes fading, it simply does not fit within the scope of this thesis.

However, as explained in Section 4.1, Morshed *et al.* defined the maximum number of available useable frequency offsets roughly based on an indoor office environment. The Friis's free-space path loss model, however, does not take this indoor office environment into account as it is defined for free space and therefore has a different path-loss exponent. Extending Friis's free-space path loss model to the log-distance pathloss allows for the use of different path loss exponents and is given by

$$L_{\mathrm{dB}} = \mathrm{PL}\left(d_0\right) + 10\alpha \log_{10}\left(\frac{d}{d_0}\right). \tag{4.9}$$

In (4.9), α is the path-loss exponent and d is the distance. $\mathrm{PL}\left(d_0\right)$ is defined as the free-space path loss at reference distance d_0, which in short-range systems, such as N-FOM in an office environment, is approximately 1 m [34]. This results in

$$L_{\mathrm{dB}} = 20\log_{10}\left(\frac{\lambda}{4\pi}\right) + 10\alpha\log_{10}\left(d\right), \tag{4.10}$$

which equals to

$$L = \left(\frac{4\pi d^{\left(\frac{\alpha}{2}\right)}}{\lambda}\right)^2. \tag{4.11}$$

Here it is assumed that communication is done on a single floor and no walls or floors/ceilings are penetrated between transmitter and receiver, i.e. there are no wall absorption losses. As it is an office environment, the path-loss exponent is assumed to be approximately $\alpha = 3.3$ [35]–[37].

4.2.4 Model implementation

The N-FOM physical layer is implemented in OMNeT++ and MiXiM as an extention to the base physical layer, as depicted in Figure 4.1, as follows. From the base physical layer a transmission power P_x is selected at the start of the simulation. This signal is sent through the FSPL channel and received as:

$$P_r = \frac{P_x}{L}. \tag{4.12}$$

Based on this an SNR per bit (γ) has to be generated. However as TR-MAC and N-FOM are built as modules in the MiXiM package, they are required to extend MiXiM's basic functions in order to maintain the ability to interchange physical layers and MAC-layers. To calculate the SNR per bit, an extension has thus been written on top of MiXiM's basic physical layer and thereby extending MiXiM's basic SNR function which actually provides the CNR of a transmitting node directly after reception. This CNR is calculated as

$$\mathrm{CNR} = \frac{P_r}{P_n} = \frac{P_x/L}{N_0 B_{\mathrm{ss}}}, \tag{4.13}$$

whereas γ is defined as

$$\gamma = \frac{E_{\mathrm{b}}}{N_0}. \tag{4.14}$$

In order to calculate the SNR per bit (γ) based of MiXiM's standard CNR function a conversion has to be made. Since $E_\mathrm{b} = P_r T_\mathrm{b}$ is the received bit energy, where T_b is the bit transmission time, it can be solved that

$$\mathrm{CNR} = \frac{P_r}{N_0 B_\mathrm{ss}} = \frac{P_r T_\mathrm{b}}{N_0 B_\mathrm{ss} T_\mathrm{b}} = \frac{E_\mathrm{b}}{N_0 \frac{B_\mathrm{ss}}{R_\mathrm{b}}} = \frac{\gamma}{S}, \tag{4.15}$$

where R_b is the bitrate and S is the spreading factor. In other words, γ can be obtained by multiplying the SNR calculated through MiXiM by the spreading factor. This calculation is performed for each concurrent active link present during the transmission period of the desired node. Based on the SNRs per bit calculated for each concurrent transmitter and selecting an appropriate spreading factor (S), SNR_l is calculated using (2.5). Depending on the number of concurrent active links, extra conditions apply for the summations performed in the denominator, adding additional noise (cross-)products. This SNR_l function thus describes the SNR per bit after demodulation and mixing. Using SNR_l the BER is calculated and checked using the packet error probability function (4.7) as described in Section 4.2.2, to determine whether or not the packet is lost due to bit errors induced during packet transmissions. This results in a different simulation model block diagram than shown in Figure 4.1, an updated version of the simulation model block diagram is depicted in Figure 4.4.

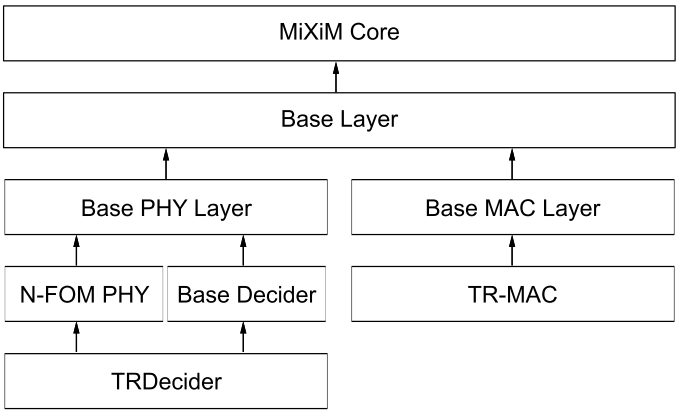

Figure 4.4: Simulation model block diagram of MAC and N-FOM physical layer implementation in MiXiM

It should be noted that the physical-layer model of N-FOM is designed in such a way that it is treated as a separate block in the simulator and has no direct link to Morshed's TR-MAC model design. The physical layer as well as the MAC layer can thus be swapped out for other models. This is advantageous as this also allows for testing N-FOM with MAC protocols other than TR-MAC and vice versa. However,

within the scope of this thesis, simulations performed will primarily cover N-FOM and TR-MAC interaction scenarios for as well peer-to-peer as MA communications.

4.2.5 Clear Channel Assessment

As explained in Section 4.1 nodes will move to the SLEEP state for a random duration if any communication was detected during the CLEAR_CHANNEL_ASSESSMENT state. Originally in Morshed's design this occured at any form of activity in the channel, resulting in the fact that only a single transmitter is allowed to transmit transmit at a specific transmission opportunity; blocking out the possibility of concurrent transmissions. However, in the case of N-FOM, a signal can still properly be received if concurrent active links are present, as every transmitter has a unique frequency offset. This, given the signals of these transmitters are sufficiently weak enough with respect to the transmission of interest. In order to determine the influence of the mixing products introduced by (2.5), the CLEAR_CHANNEL_ASSESSMENT state thus has to be altered. In order to do so a threshold has been implemented in the physical layer, where nodes in the CLEAR_CHANNEL_ASSESSMENT state check if the SNR of the signal in the channel received is below a specific value. This threshold is based on theoretical analysis on how the SNR per bit of a specific transmitter influences the BER of the received signal of the node of interest. This is depicted in Figure 4.5.

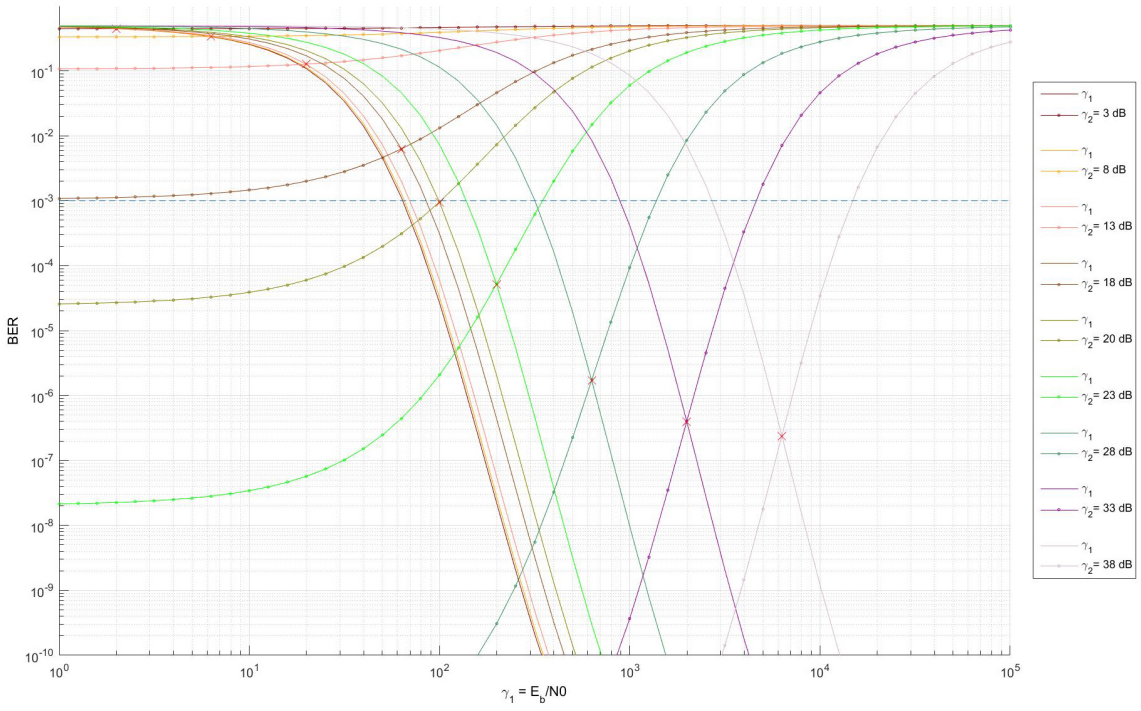

Figure 4.5: BER of two users as a function of γ_1, with $S = 200$.

In the scenario of Figure 4.5 it is considered that there is a receiver simultaneously listening to two transmitting users using different frequency offsets. In this case the SNR per bit of User 2 (γ_2) is fixed for different values and the BER of both users is plotted as a function of the SNR per bit of User 1 (γ_1). Here, User 1 is the node of interest and User 2 is an interfering node. It is evident that the BER of User 2 deteriorates when the SNR per bit of User 1 increases, improving the BER of User 1. Mathematically, this relation can be defined as

$$\mathrm{BER} = Q\left(\sqrt{\mathrm{SNR}}\right),\ \mathrm{SNR} = \frac{8\gamma_1^2}{\left(25\gamma_1^2 + 17\gamma_2^2 + 20\gamma_1\gamma_2\right)/S + \left(20\gamma_1 + 16\gamma_2\right) + 8S}, \tag{4.16}$$

where the SNR in (4.16) is a simplification of (2.5). Given that a proper signal reception for User 1 is desired – as a general rule of thumb this means a BER lower than 10^{-3} – whereas the signal of User 2 is desired to have the least amount of influence as possible – i.e. a BER higher than 10^{-3}, a maximum SNR per bit of User 2 can be defined for which signal reception of User 1 can be assumed to be received correctly a significant amount of the time. In Figure 4.5, cross-sections are indicated and compared to the theoretical BER requirement. Here it is evident that in order to have an acceptable BER for User 1, while having little influence of User 2, the SNR per bit of User 2 should be lower than 20 dB. This, assuming that the SNR of User 1 is not too weak to begin with, which is mostly not the case unless very large distances are covered. In other words

$$\gamma_2 \leq 20\ \mathrm{dB}. \tag{4.17}$$

This generalisation does not only hold for 2 concurrent transmitters. Based on Cauchy-Schwarz inequality it can be stated that if the mixing products of n amount of concurrent transmitters that are not of interest with a total SNR per bit of 20 dB has equal or less impact on the BER of User 1 than a single concurrent active transmitter's SNR per bit of 20 dB. It thus should hold that

$$\gamma_{\mathrm{mixingprod}} \leq \gamma_2 \leq 20\ \mathrm{dB}, \tag{4.18}$$

given that the noise products of (2.5) are equal to the noise products of (4.16) with a γ_2 of 20 dB for a specific value of γ_1, i.e.

$$\left(17\sum_{\substack{i=1\\ i\neq l}}^{N}\gamma_i^2 + 20\gamma_{l=1}\sum_{\substack{i=1\\ i\neq l}}^{N}\gamma_i + 16\sum_{\substack{i=1\\ i\neq l}}^{N-1}\sum_{\substack{j=i+1\\ j\neq l}}^{N}\gamma_i\gamma_j\right)\frac{1}{S} + 16\sum_{\substack{i=1\\ i\neq l}}^{N}\gamma_i = \left(2000\gamma_{l=1} + 17\cdot 10^4\right)\frac{1}{S} + 1600. \tag{4.19}$$

Simply said, if the channel is sensed and the SNR per bit of the signal directly at the antenna is lower than 20 dB, the physical layer will tell the MAC layer it can move to the SEND_DATA state, else it will back off randomly and move to the SLEEP state. It should, however, be stated that this threshold method does not account for possible near-far effects between transmitters and receivers during the CLEAR_CHANNEL_ASSESSMENT state, it could thus occur that a receiver is placed in such a way that the transmitter of interest will not transmit due to a too strong signal present whereas it would've been acceptible due to the near-far effect if the other transmitter is further away from the receiver – or vice-versa.

4.3 Conclusion

Within this chapter the combined simulation model design of N-FOM and TR-MAC has been given. A summary is given of Morshed's simulation model and of the abstractions that were implemented. Based on Morshed's simulation model, the model has been extended by incorperating the N-FOM physical layer and hard limits from the TR-MAC layer and physical layer abstractions have been removed. The physical layer has been implemented based on a high-level mathematical expression of the N-FOM physical layer in order to achieve relatively fast simulation times. The expression is directly taken from Bitachon's research as the goal of this thesis was to implement the layer, not to verify it. The MiXiM base physical layer has been extended in a separate N-FOM block to fit this expression. In order to achieve a more realistic channel model, a Bernoulli random process has been implemented as method of packet error generation. Additionally, Friis's free space path loss model has been extended to fit more realistic path-loss exponents. Based on this extended simulation model combining N-FOM and TR-MAC, simulations will be performed. Results of these simulations will be provided in Chapter 5.

Chapter 5

Simulation results

5.1 Physical layer verification

As discussed in Chapter 2, a large limitation on the physical-layer side is that if the number of concurrent active links increases the received signal BER also increases significantly due to additional noise and mixing terms generated during demodulation. In order to verify this phenomenon and to get an idea on the maximum number of active concurrent links allowed before the BER reaches unacceptible values and the received signal is saturated with noise, an initial test has been performed. For this test the physical layer as modelled by (2.5) and the channel as defined in (4.10) have been used. The MAC layer has been omitted, to prevent any regulation on communication of nodes in the network; resulting in all nodes trying to communicate at the same time.

In this simulation a single node is selected to be a receiver and an increasing number of transmitting nodes, using unique frequency offsets, are added step-by-step. For the transmitting nodes, distances are selected to be equal in respect to the receiving node, with line of sight (LOS) communication. Furthermore, the distance is selected such, that in peer-to-peer communication the SNR_l reaches its equilibrium state as discussed in Section 2.1, with as results the packet error probability is very small without mixing products of interfering nodes. This to ensure packets only have interference from mixing products from other active nodes. Distances for transmitting nodes to receiver have been chosen equal, so no near-far effect is present. Other variables are chosen such that it is according to Table 4.1 and a spreading factor of 200 has been chosen. In order to generate results, N-FOM is simulated using the MiXiM package, as discussed in Chapter 4, to generate and transmit 2000 packets at each transmitter. From this simulation the total number of dropped packets due to interference, i.e. mixing products, is divided by the total number of transmitted packets to give a percentage of accepted and dropped packets for a specific number of concurrent active transmitters. Results are given in Figure 5.1.

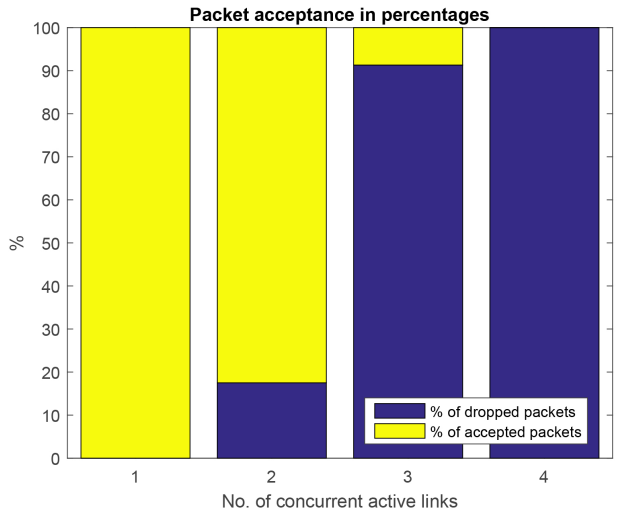

Figure 5.1: Packet acceptance in "physical layer only" interaction with increasing number of concurrent active links, where $d = 3$ m, $\alpha = 3.3$, $\mathrm{P_t} = 2$ mW, and $S = 200$.

As apparent from Figure 5.1, the percentage of dropped packets significantly increases with more than two concurrent active links simultaneously trying to communicate to the same node; at least 90% of the packets drop due to interfering nodes. At four or more concurrent active links the mixing noise products are predominantly present and all information is lost. As the concept of N-FOM is to use it in an MA environment, it is expected that more nodes will be present than the four only tested so far. It is thus clear the mixing products severely limit the performance of N-FOM without proper medium access control. It should thus be made sure that at all times a maximum of two nodes are concurrently active in order to maintain a proper packet acceptance rate. Morshed's TR-MAC design should do just this, but needs to be validated with N-FOM as discussed in Chapter 3 and Chapter 4. However, first it should be verified that the stochastic validation process discussed in Section 4.2.2 is implemented correctly. This is discussed in Section 5.2.

5.2 Peer-to-peer model testing

Because of the limitations of N-FOM as result of its self-mixing behavior, Morshed designed TR-MAC as a viable MAC protocol to work with N-FOM in MA environments [16]. However, as stated in Chapter 3, the MAC layer was only tested though simulation in conjunction with an abstraction of a physical layer and required further analysis. Due to the frequency allocation method used in TR-MAC, as discussed in Section 3.3, it is expected that peer-to-peer communication occurs most often and

cross-mixing of concurrent active links is not always present. It is therefore important to ascertain that the N-FOM physical layer simulation model is working correctly in conjunction with TR-MAC in single transmitter-receiver communication and the validation process used has outcomes that do not deviate too much from the theoretical values.

For the peer-to-peer simulation a single node is selected as receiver and a single transmitter is set at predetermined distances in LOS from the receiving node, such that the theoretical packet error probabilities are 0, 30, 50, 70, and 100 percent respectively. Futhermore, receiver sensitivy limitations are disabled in order to make sure only the possible deviation of the transmission success process described in Section 4.2.2 is measured. Other variables are again chosen such that it confers with Table 4.1, with a spreading factor of 200, a pathloss exponent of 3.3 and the physical layer modeled as discussed in Chapter 4, to generate and transmit 4000 packets at the transmitter. Within this simulation, the number of dropped packets at the receiver is divided by the total number of packets received to calculate the percentage of failed packets. Results are given in Figure 5.2(a) and Figure 5.2(b).

In Figure 5.2(a) the percentual packet error pobability is given with 99.9% confidence interval (CI). The confidence interval was calculated as

$$\bar{X} \pm z^* \frac{\sigma}{\sqrt{n}}, \tag{5.1}$$

where $\bar{X}$ is the sample mean, σ is the sample standard deviation, n the sample size, and z^* the z-value. Here the sample mean is calculated as

$$\bar{X} = \frac{1}{n} \sum_{i=1}^{N} X_i, \tag{5.2}$$

and the standard deviation as

$$\sigma = \sqrt{\frac{1}{n-1} \sum_{i=1}^{N} \left(X_i - \bar{X}\right)^2}. \tag{5.3}$$

From this figure it can be seen that simulation follows theory relatively well. At a CI of 99.9% all measurements fall within the values calculated by theory. The theoretical value of 50% packet error probility has slightly better performance, whereas at 10% packet error probability there is slightly less performance. Given there is a 99.9% confidence interval used, there is a 0.1% chance deviations occur outside of the measured values. Therefore, the implementation done in simulation deviates slightly form theory, which could be due to the way the packet error probabilities are defined

and calculated, as it is still an approximation. However, it can be stated that the deviations observed are not significant enough to assume the transmission success process used is invalid.

Figure 5.2(b) depicts the packet error probability on a logarithmic scale. Here it can be observed that the packet error probability simulation plot (and its deviations) closely follows the curve of the BER plotted against the SNR per bit in [17]. This acts as an alternative presentation in percentages for better overview in probabilities. Hence, it can be concluded that the N-FOM physical layer is implemented properly enough in the simulator, allowing for further and more extensive testing of N-FOM on the TR-MAC-layer.

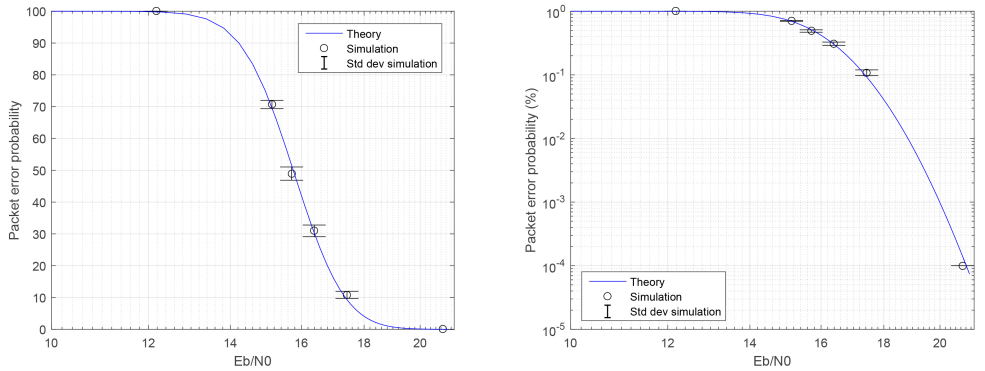

(a) percentual packet error probability with 99.9% CI

(b) logarithmic packet error probability with 99.9% CI

Figure 5.2: Package error probability plotted against SNR per bit at a 99.9% CI from simulation in respect to theory, where $\alpha = 3.3$, $P_t = 2$ mW, and $S = 200$.

5.3 Multiple access modelling

As became apparent from Chapter 3 and Section 5.2, peer-to-peer communication is the most common form of communication in TR-MAC, where only one concurrent transmitters is present, as in synchronized links nodes are given a non-overlapping wake-up time based on their uniquely allocated frequency offset out of a pool of 25. Additionally, channel sensing prevents concurrent transmissions as when the channel is sensed busy, transmitters simply back off. In Section 5.2 it has been shown that peer-to-peer is working as expected and does not show any abnormal behavior at conditions where the packet error probability increases. In order to see the limitations of TR-MAC in MA, Morshed tested the throughput of the system when the number of concurrent active nodes increases, as depicted in Figure 3.3. Morshed concluded that if the number of concurrent active links increases, throughput collapses as the maximum number of concurent active links exceeded the main

limitation invoked by the N-FOM physical layer as shown in Figure 5.1. However, Morshed used a basic physical-layer model where hard limites were set, using a threshold on CNR at reception as well as on the maximum number of concurrent active links. Morshed did thus not implement the physical layer according to (2.5), but used abstractions instead.

5.3.1 Throughput performance

As the N-FOM physical layer differs significantly from the abstractions Morshed used, in terms of contributed noise through the channel as well as the mixing products from demodulation, it is interesting to see whether or not the throughput behaviour changes and if the decay occurs with a lesser number of nodes present. For this measurement the same receiver-driven stategy as used by Morshed is chosen, where a single receiver can pair with up to 25 transmitters using 25 different frequency offsets. The number of active links in the network will start with 25 and will be increased gradually until saturation occurs. Results are given in Figure 5.3(a) and Figure 5.3(b).

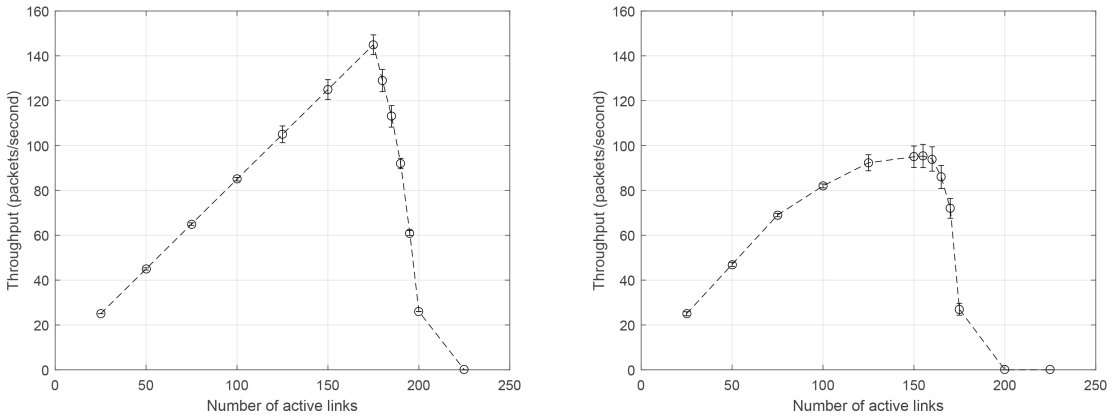

(a) Throughput performance for varying number of active links distributed over a small area

(b) Throughput performance for varying number of active links distributed over a large area

Figure 5.3: Throughput performance for varying number of active links using TR-MAC in conjunction with the N-FOM physical layer, where $\alpha = 3.3$, $\mathrm{P_t} = 2$ mW, and $S = 200$.

In Figure 5.3(a) the throughput is plotted over the number of active links distributed over a relatively small area. Nodes are uniformly distributed, i.e. every node can be put at any location in that area with the same likelyhood, over an area where the probability that they are in each others' transmission range is significantly large.

This also means the near-far effect is present. Here it can be seen the throughput increases linearly with the increase of active links and then experiences a hard drop. The reason for the linear increase in throughput until 175 active links is attributed to the fact that every transmitters performs clear channel assessment (CCA) and backs off if the channel is sensed busy. As a results primarily only one link is active most of the time reducing the physical layer from (2.5) to (2.4), removing cross-noise mixing terms from the equation. This means the receiver has full control of its sender pairs in the receiver-driven communication strategy as also explained in [16], allowing to establish synchronized links as explained in Chapters 3 and 4. When compared to Figure 3.3, it can be seen the increase is also linear, but not as steep. This is due to the fact that in N-FOM the SNR per bit is significantly greater than the SNR calculated in [16], causing nodes to back off more often as the channel is sensed busy, reducing throughput.

The sudden drop in throughput performance depicted in Figure 5.3(a) is observed from 175 active links. This is due to the fact that more and more transmitters will back off as they sense the channel is busy due to an increasing number of concurrent active links per receiving node, resulting in the scenario where the system eventually falls back to where a single transmitter receiver pair is active at a specific timeslot, as can be seen at 200 nodes. There is thus a high probability that most, if not all, concurrent active transmissions fail. As a result, the throughput drops significantly. It would have been expected that the throuhput for more than 200 nodes would become constant due to the fact that a bottleneck would have been reached where only one transmitter transmits at a specific time due to the CCA operation, where every other node senses the channel is busy. However, as can be seen the throughput becomes zero, although the exact reasons for this is not exactly clear it is assumed this is due to the fact that nodes lose synchronisation as they cannot communicate with their pair, but are also unable to form new pairs as the channel is always sensed busy, eventually resulting in a deadlock.

In Figure 5.3(b), the throughput is plotted over the number of active links distributed over a relatively large area. Here the area where the nodes are uniformly distributed over is significantly larger. Nodes can easily be placed far out of the range of other nodes, allowing for the possibility of hidden terminal effects. In order to prevent receivers unable to form pairs, however, it is modelled that every receiver has 25 transmitters nearby to synchronize with. This in order to prevent additional loss in throughput due to artifacts as a result of discontinuety in the network. It is apparent fom this figure that the increase in throughput is no longer linear but becomes saturated as the number of nodes increases. This is most likely attributed due to the hidden-terminal effect. As nodes trying to transmit to their synchronized receiver pair can be far enough away from each other not being able to sense them during

their CCA state, whereas the receivers can be closeby enough that their reception causes interference on the other receiver increasing cross-mixing products at both receivers. As a result, there is a higher probability packets will be dropped earlier due to an overall increase in the BER. Furthermore, it can be seen that the decay in throughput occurs earlier than in Figure 5.3(a), with a steeper decline. This is most likely due to the fact that not only more nodes enter the network and thus nodes back off more often at their CCA state, but also more nodes start to consistently fail due to high packet error probabilities if they are allowed to transmit. As a result less packets arrive properly at the receiver and the throughput decreases.

5.3.2 Throughput performance with adjusted clear channel assessment

In order to see the effects of the squaring operation, the CCA state as discussed in Chapter 4.2.5 has been adjusted to allow concurrent active transmissions if overall sensed power in the channel allows for it in order to prevent direct colissions. If the channel is too heavily occupied, the node will randomly back off according to the CCA explained in Section 4.1 Measurements have been performed the same as for Figures 5.3(a) and 5.3(b). Results are given in Figure 5.4(a) and Figure 5.4(b).

In Figure 5.4(a) the throughput is again plotted over the number of active links distributed over a relatively small area. Nodes are uniformly distributed, over an area where the probability that they are in each others' transmission range is significantly large. It can be seen the throughput no longer increases linearly as in Figure 5.3(a) but has a roughly linear increase up to 75 nodes and then saturates with increasing numbers of active links and then experiences a hard drop. The reason for the increase in throughput at the lower number of active links is attributed to the fact that the receiver has full control of its sender pairs and no concurrent transmissions are occuring. However, given that receivers are not synchronized to one another, it can be concluded that the periodic listen cycles per receiver are independent of each other, thus also the time instances allocated by a receiver per frequency offset. It could thus occur that for specific time instances there is overlap due to concurrent transmissions using different frequency offsets, however, the N-FOM is able to cope with this to a certain extent. However, when the number of active links increases, the probability increases that more concurent transmissions occur. These concurrent transmissions result in additional mixing terms in the receiver due to self-correlation, roughly causing a quadratic increase in noise, resulting in higher packet error probabilities. In other words, the throughput no longer has a linear increase if more mixing terms are present. This phenomenon occurs primarily at more than 100 active links present.

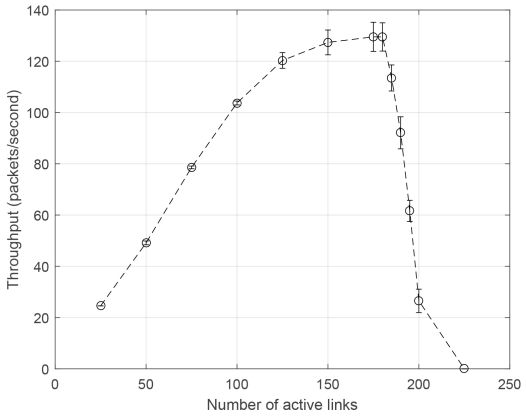

(a) Throughput performance for varying number of active links distributed over a small area

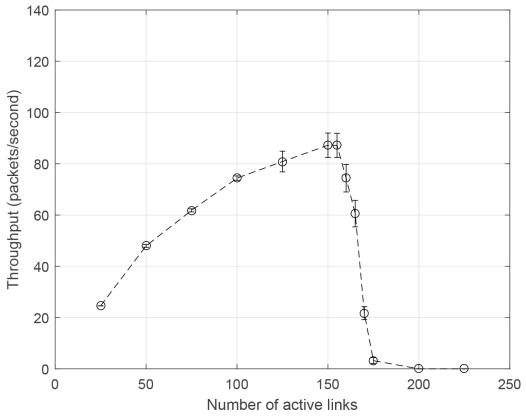

(b) Throughput performance for varying number of active links distributed over a large area

Figure 5.4: Throughput performance for varying number of active links using TR-MAC in conjunction with the N-FOM physical layer using the adjusted clear channel assessment, where $\alpha = 3.3$, $\mathrm{P_t} = 2$ mW, and $S = 200$.

The sudden drop in throughput performance depicted in Figure 5.4(a) is observed from 175 active links, the same as Figure 5.3(a). This is logical as the same CCA method applies as originally implemented when too many links want to be concurrently active.

In Figure 5.4(b), the throughput is again plotted over the number of active links distributed over a relatively large area. Again allowing for the possibility of hidden terminal effects. It is apparent fom this figure that the decay in throughput occurs earlier than in Figure 5.4(a). This is logical as the CCA cannot cope with hidden terminal effects. Resulting in a faster saturation in throughput. The decline is also steeper similar to Figure 5.3(b). This is also most likely due to the fact of a combination of channel contention and high packet error probability rates.

5.3.3 Throughput performance comparison

A comparison of system throughputs with Morshed's performance model are plotted in Figures 5.5(a) and 5.5(b). From these figures it can be observed that with the N-FOM physical layer the thoughput achieved is less than Morshed originally expected. For the simulations performed where nodes are distributed over a small area (Figure 5.5(a)) it is evident there is a tradeoff between the standard CCA method and the adjusted CCA as explained in Section 4.2.5. For a lower number of active links in the network it is more favorable to allow for concurrent transmissions as the receivers can easily cope with it. As a result, fewer transmitters have to back off during

CCA and higher thoughput is achieved, whereas in the case of the previously implemented CCA used more nodes where forced to back off resulting in a reduced throughput. In the case of a higher number of active links, however, mixing products start taking the overhand. In this case the old CCA method is preferable as higher throughput is reached. This only does not last long as both methods result in severe degredation in throughput as too many links are present. However, it can be stated that most of the time the new CCA approach if more effective

In the case of Figure 5.5(b), it is easily observed the presence of hidden terminals cause sever degredation in throughput for both CCA methods, as noise terms quadratically increase. However, the old CCA method proves slightly more efficient as the new implementation allows for more concurrent transmissions. Hence the use of concurrent transmissions uneffective in applications where nodes are distributed over a large area.

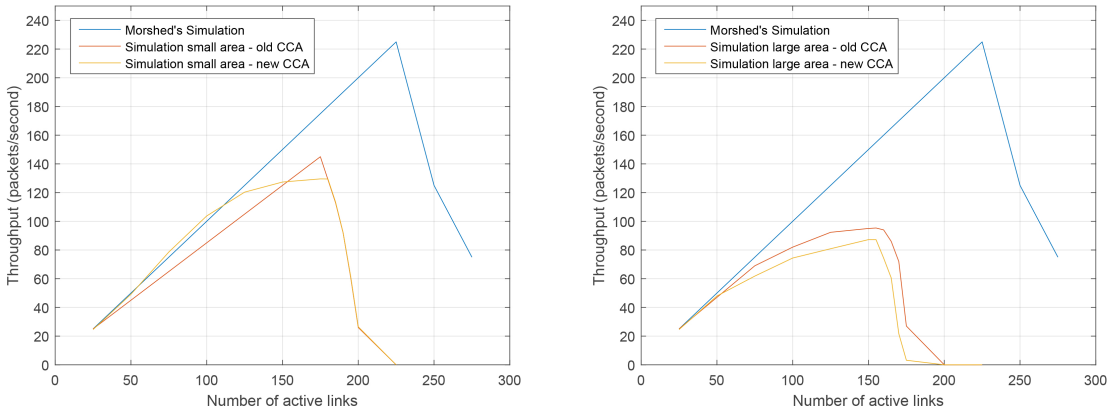

(a) Throughput performance for varying number of active links distributed over a small area

(b) Throughput performance for varying number of active links distributed over a large area

Figure 5.5: Throughput comparison between simulations results in small and large areas with respect to Morshed's throughput performance model.

Although results shown in this section reveal that the throuhput performance is less that initially expected, it should be taken into account those measurements were performed with a very simple physical layer. With the N-FOM physical layer implemented a lot of factors weigh in on how the system performs. There is thus a probibility that by tweaking the parameters used in the physical layer, a throughput performance can be obtained that is closer to Morshed's result.

5.3.4 Throughput performance with changes in physical layer

As previous measurements have shown the physical layer does influence the performance of the system and that it is visible at the MAC level, it is interesting to see how changes in the physical layer influence this behavior. For purpose an additional measurement has been performed with the same set up as in Sections 5.3.1, 5.3.2, and 5.3.3 for nodes uniformly distributed over a small area using the adjusted CCA state. However, this time the spreading factor has been increased from 200 to 1000 and is then compared to the situation where the spreading factor was 200. The result in shown in Figure 5.6.

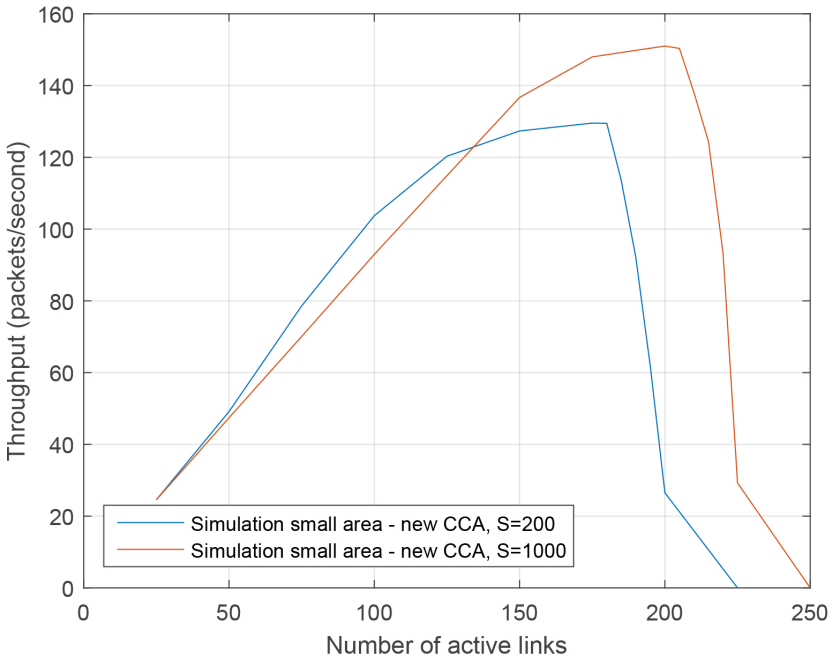

Figure 5.6: Throughput comparison between simulations results in small areas with different spreadin factors., where $\alpha = 3.3$ and $P_t = 2$ mW.

In Figure 5.6, it can be seen that changing the spreading factor does indeed influence the throughput behavior of the system. The has a more linear behavior up to 150 active links and then starts to saturate, in contract to the case where the spreading factor was 200, here saturation started at 75 active links. Additionally, higher throughputs are achieved for higher number of links and there's a later decline in performance. However, the throughput performance in the lower number of active link regime is slightly worse. This is logical, as when looking at (2.5) it can be seen that if the spreading factor increases, mixing terms are supressed, resulting in less saturation in the network due to concurrent transmissions. However, the

in-band noise increases, as a result the slope of the linear increase in throughput for a lower number of active links decreases due to a lesser signal performance.

When looking at the overall decline in throughput, this occurs later than when the spreading factor was 200. As the signals have less interference from mixing terms it is better able to cope with concurrent transmissions, resulting in the fact that more concurrent active links have to be present for nodes to be forced to back-off in the CCA phase. As a result throughput will start to decline at roughly 205 concurrent active links instead of 175. It can thus be stated that the overall performance of the N-FOM physical layer in conjunction with the adapted CCA state and TR-MAC is better for higher values of the spreading factor. It should however be noted that if a lot of in-band interference are present, it is more favorable to keep the spreading factor low, as that could also have significant influence on the system (see Section 2.2.3).

5.4 Simulator efficiency

Given that the physical layer model is implemented based on a higher level theoretical approximation of the N-FOM physical layer scheme, instead of modeling it on bit level, simulator performance should be significantly faster. In order to define how efficient the simulator is, the CPU time has been measured using the Linux `time` function. Results are given in Figures 5.7(a) and 5.7(b). From Figure 5.7(a), simulations have been performed in the same way as the above multiple access measurements were done for nodes distributed over a small area. All nodes were put into the area at the same time. It can be observed that for a low number of nodes, simulation time is relatively fast, approximately 10 seconds. However, when increasing the number of active links the simulation time increases exponentially, up to roughly 1.5 hours for 250 nodes. This is primarily due to the unsynchronized link state of the MAC layer. Given that all nodes entered the area at the same time they all try to communicate at the same time to a receiver using small preamble bursts and repeat this for the full timeslot receivers can utilize to wake up and communicate to nodes. Given that the CCA will force all nodes into back off with random timers, nodes will repeat this process until all nodes achieved synchronized links. As only one node can be active on the unsynchronized frequency offset, nodes will be forced to back off a lot and synchronization takes very long.

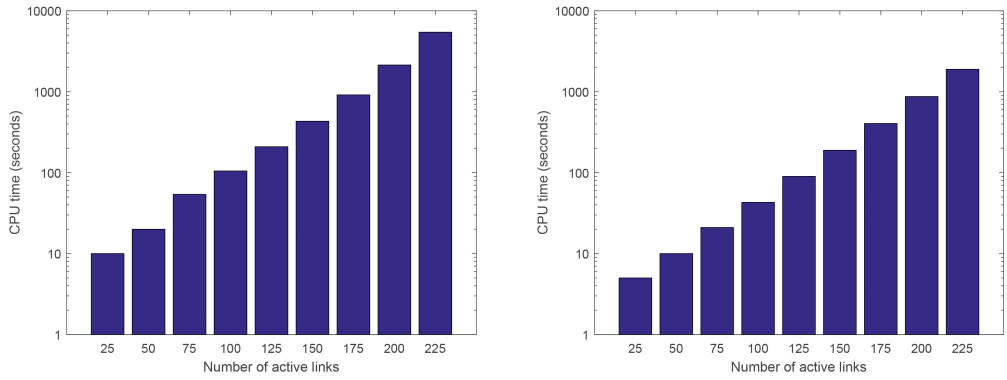

(a) CPU Time of simulation with all nodes initialized at the same time

(b) CPU Time of simulation with all nodes initialized one after each other

Figure 5.7: Measurement of CPU time for simulation with an increasing number of active links.

In Figure 5.7(b) the same simulation has been performed except that nodes are initialized one-by-one to prevent uneccessary channel contention during the unsynchronized link state. As can be seen this reduces simulation time significantly where 250 concurrent active links now only take 30 minutes to simulate. However, back offs during unsynchronized link still occured due to channel contention.

When looking at the overal efficiency of the simulator it is hard to tell whether or not the simulator is as efficient in timing as it could be. Simulator efficiency is relative in the sense that high-level implementations are supposed to take a fraction of the low-level implementation to be efficient. In the case of N-FOM low-level simulator times are not yet measured. This needs to be investigated further in order to determine the overall efficiency of the simulator system made in MiXiM.

5.5 Simulator Limitations

Due to the fact the simulator has been built MiXiM, which is a deprecated package that no is longer supported, is that some limitations come with it. The primary limitation of the design of a simulation program in MiXiM being the lack of documentation and updates. Given that MiXiM is built as an package for OMNeT++, it utilizes initialization files to define simulator characteristics, e.g. sensitivity, resolution, etc. However, due to the lack of documentation it is very hard to define what variable define what. Furthermore, not all functions used in MiXiM still function properly with newer versions of OMNeT++ and operating systems. Additionally, as MiXiM was originally used as a scientific package for specific universities and research institutes it is primarily designed for internal used by employees of the respective organizations. As

a results multiple organizations built sub-parts of the package resulting in the lack of structure, organization and stability. Although MiXiM is a very helpful and a powerful tool in design and implementation of a full network simulation, it comes with a steep learning curve, and requires time to grasp. Due to lack of documentation and the steep learning curve, significant time was spent on making the simulator. Better would have been to use INET, MiXiM's successor, as it is more properly documented and structured. However, as TR-MAC was made in MiXiM, and INET is not backwards compatible, this was not possible as redesigning the MAC layer did not fit within the scope of this thesis. It is, however, recommended that for future work on this project a different simulator package is used.

5.6 Conclusion

Within this chapter the simulation results of the combined N-FOM and TR-MAC simulation model have been presented. Four types of measurements have been performed: physical layer verification; peer-to-peer communication testing; MA simulations; and simulator efficiency testing. Verifications testing for the physical layer has shown the limitations found match that of the theory. In peer-to-peer communication the physical layer has been tested in conjunction with the MAC layer and proper implementation has been verified. Measurement results from MA simulations have shown that the physical layer has influence on the results obtained at MAC level which were previously not accounted for. Throughput estimation was too optimistic and mixing terms saturate throughput performance due to quadratic increase in noise. For a high number of nodes throughput declines due to channel contention. Additionally, different parameter settings in the physical layer yield different result at the MAC level, which needs to be further investigated. Simulator efficiency measurements also have been performed. Concurrent initialization of nodes significantly reduces speed due to the preable stage in the unsynchronized link state. Initializing nodes one after another yields faster results. The overall efficiency of the simulator in terms of speed still needs to be evaluated as no time measurements of low-level physical layer models have been performed yet. Furthermore, the limitations of the simulation package used have been described.

Chapter 6

Conclusions and recommendations

6.1 Conclusions

In this thesis, a combined simulation model of N-FOM and TR-MAC has been made. N-FOM and TR-MAC have both seperately been investigated in performance, strength and weaknesses. The total performance of the combined system has been evaluated and compared to Morshed's simulation model using the combined N-FOM and TR-MAC simulation model. (In previous simulation of TR-MAC, the N-FOM physical layer has not been considered yet.) Morshed's simulation was extended with the N-FOM physical layer and results show the implemented physical layer functions according to theory. Depending on the way CCA is implemented throughput performance changes. In the CCA scenario where transmitters back off if the channel is sensed busy by another node, throughput performance is linear, yet not as steep as expected, but yields slightly better throughput for a higher number of concurrent active links. For a CCA where multiple concurrent links are allowed depending on how powerful they are, throughput performance is slightly better for lower number of active links but saturates for when the number of active links increases. In a multi-user environment, it has thus been shown that the self-correlation receiver has significant impact on the throughput of the system in a LOS environment due to addition mixing products induced by concurrent active links. The increase in throughput is no longer linear as Morshed initially expected, but saturates. Additionally, the sudden decay in throughput as an effect of more concurrent active links in the network is steeper than previously anticipated. Additionally, increasing the spreading factor for a multipath environment yields better throughput for a higher number of active links, however, overall in-band noise increases. So a trade-off in performance is present. The effects due to the self-correlation receiver had not previously been accounted for in the testing and validation of TR-MAC design. An improvement could be to update the `CLEAR_CHANNEL_ASSESSMENT` state of the TR-MAC protocol, to where it not only checks whether or not the channel is proper enough for transmissions,

but actually checks the preamble based on the transmitter's own and two closest neighbouring frequency offsets to prevent overlapping transmission opportunities due to unsynchronized clocks. This should already lower the noise contribution of the self-correlation receiver to a significant extent as the probability of two overlapping transmissions that have a higher likelihood to interfere with each other is reduced significantly.

Based on the findings of the simulation results, it can be concluded that the simulator is suitable as a basis for more extensively testing the influences of the physical layer on the MAC layer, as physical layer phenomena effects can now be clearly simulated.

6.2 Recommendations

Given that N-FOM was primarily designed for use in multi-path (MP) environments, the simulation can now be extended to incorperate those. This did not fall within the scope of this thesis as a closed form expression of the N-FOM MA MP model was not available at the time. It should, however, be noted that the current tests performed in LOS are primarily done for analysis purposes than for real practical implementation, as there is already a standard greater than 10.8 dB loss at the receiver and most likely does not outperform any standard system used for WSNs. Although incorperation of channel coding could improve the system a bit, it would be more interesting to see how N-FOM and TR-MAC performs in MP environments where it should have an advantage as it can exploit channel diversity.

Due to the lack of a N-FOM multipath model available at the time of this Master's thesis, only the implementation of N-FOM in LOS with relatively simple pathloss model could be facilitated. This only allowed for validating the simulator in terms of physical layer implementation instead of showing the full impact of the physical layer on the MAC-layer. Although it is proven in this thesis that it is very well feasible to properly implement a simple physical layer model conjunction with the MAC layer model in simulation, and still have the possibility to perform swift simulation runs, further research and work is required to define a mathematical physical layer model that incorporates multipath phenomena for multiple access communication in N-FOM and implement it accordingly. Only after doing so, the full influence of N-FOM, and the possible gains that come with it in an LOS environment, can be simulated and tested.

Furthermore, improving the `CLEAR_CHANNEL_ASSESSMENT` state in the MAC layer should also give better outcomes for throughput in MA with the N-FOM physical layer. Having transmitters quickly check the short preambles for frequency offsets that are the same as, or close to the one used in, the transmitter performing the

assessment could reduce the noise contribution by the self-correlation receiver to a certain extent. Implementing channel coding in the MAC layer should also help reducing the $\geq$10.8 dB loss inherently present in the N-FOM physical layer.

Additionally, the use of the depricated mixed simulater framework MiXiM, although effective for easy MAC implementation, has proven to give great difficulties in facilitating the physical layer. The package relies on a lot of old software libraries, of which some give problematic outcomes depending on the operating system. Additionally, due to the lack of documentation the learning curve for MiXiM is very steep. It is therefore not suggested to continue modelling the N-FOM and TR-MAC simulation environment with this package, but rather start over from scratch and properly document it, or use a properly documented framework to begin with.

Bibliography

[1] L. S. Rensen and K. E. Skouby, “User scenarios 2020 - a worldwide wireless future,” *OUTLOOK Visions and research directions for the Wireless World*, 2009.

[2] S. Sheng, L. Lynn, J. Peroulas, K. Stone, I. O’Donnell, and R. Brodersen, “A low-power CMOS chipset for spread spectrum communications,” in *1996 IEEE International Solid-State Circuits Conference. Digest of Technical Papers, ISSCC*, San Francisco, CA, USA, Feb. 1996, pp. 346–347.

[3] M. Z. Win, “A unified spectral analysis of generalized time-hopping spread-spectrum signals in the presence of timing jitter,” *IEEE Journal on Selected Areas in Communications*, vol. 20, no. 9, pp. 1664–1676, Dec. 2002.

[4] S. J. Kim, C. S. Park, and S. G. Lee, “A 2.4-GHz ternary sequence spread spectrum OOK transceiver for reliable and ultra-low power sensor network applications,” *IEEE Transactions on Circuits and Systems I: Regular Papers*, vol. 64, no. 11, pp. 2976–2987, Nov. 2017.

[5] M. Z. Win and R. A. Scholtz, “Ultra-wide bandwidth time-hopping spread-spectrum impulse radio for wireless multiple-access communications,” *IEEE Transactions on Communications*, vol. 48, no. 4, pp. 679–689, Apr. 2000.

[6] C. Cook and H. Marsh, “An introduction to spread spectrum,” *IEEE Communications Magazine*, vol. 21, no. 2, Mar. 1983.

[7] U. Madhow and M. L. Honig, “MMSE interference suppression for direct-sequence spread-spectrum CDMA,” *IEEE Transactions on Communications*, vol. 42, no. 12, pp. 3178–3188, Dec. 1994.

[8] Z. Xie, R. T. Short, and C. K. Rushforth, “A family of suboptimum detectors for coherent multiuser communications,” *IEEE Journal on Selected Areas in Communications*, vol. 8, no. 4, pp. 683–690, May. 1990.

[9] M. Z. Win and R. A. Scholtz, “On the energy capture of ultrawide bandwidth signals in dense multipath environments,” *IEEE Communications Letters*, vol. 2, no. 9, pp. 245–247, Sep. 1998.

[10] F. Adachi, M. Sawahashi, and H. Suda, "Wideband DS-CDMA for next-generation mobile communications systems," *IEEE Communications Magazine*, vol. 36, no. 9, pp. 56–69, Sep. 1998.

[11] D. Cassioli, M. Z. Win, F. Vatalaro, and A. F. Molisch, "Performance of low-complexity RAKE reception in a realistic UWB channel," in *2002 IEEE International Conference on Communications. Conference Proceedings. ICC 2002 (Cat. No.02CH37333)*, vol. 2, New York, NY, USA, USA, Apr/May. 2002, pp. 763–767 vol.2.

[12] R. T. Hoctor and H. W. Tomlinson, "An overview of delay-hopped, transmitted-reference RF communications," *GE Research & Development Center – Technical Information Series*, 2002.

[13] J. Haartsen, X. Shang, J. Balkema, A. Meijerink, and J. Tauritz, "A new wireless modulation scheme based on frequency-offset," *12th Annual Symposium of the IEEE/CVT, Benelux Chapter*, 2005.

[14] I. Bilal, A. Meijerink, and M. J. Bentum, "Analysis of In-band Interference in Noise-based Frequency Offset Modulation," *IEEE 25th Annual International Symposium on Personal, Indoor and Mobile Radio Communications, PIMRC*, Sep. 2014.

[15] S. Morshed and G. Heijenk, "TR-MAC: An Energy-Efficient MAC Protocol for Wireless Sensor Networks Exploiting Noise-based Transmitted Reference Modulation," *2nd Joint ERCIM eMobility and MobiSense Workshop*, 2013.

[16] S. Morshed, "Energy-efficient medium access control for transmit reference modulation," Ph.D. dissertation, University of Twente, 2017.

[17] B. I. Bitachon, I. Bilal, A. Meijerink, and M. J. Bentum, "Near-Far Problem in Noise-based Frequency-Offset Modulation," *Communications and Vehicular Technology in the Benelux (SCVT)*, Nov. 2015.

[18] I. Bilal, A. Meijerink, and M. J. Bentum, "Optimum Receiver Filter for a Noise-based Frequency-Offset Modulation System," *Personal, Indoor, and Mobile Radio Communications (PIMRC)*, 2016.

[19] ——, "Performance Analysis of Noise-based Frequency Offset Modulation in Dense Frequency-Selective Fading Channels," *Signal Processing and Communication Systems (ICSPCS)*, 2016.

[20] ——, "Single-tone Interference in Noise-based Frequency Offset Modulation," *21st Annual Symp. of the IEEE/SCVT Benelux Chapter*, Nov. 2014.

[21] I. Bilal, “Noise-Based Frequency-Offset Modulation (title subject to change)–excerpt from draft thesis,” Ph.D. dissertation, University of Twente, 2017.

[22] A. Bensky, *Wireless Positioning Technologies and Applications, Second Edition*. Artech House, 2016.

[23] X. Shang, “New radio multiple access technique based on frequency offset division multiple access,” Master’s thesis, University of Twente.

[24] C. V. N. Bhaskar, K. J. S. Lorraine, and D. V. Ratnam, “Analysis of Near-Far Problem using Power Control Technique for GNSS based Applications,” *International Journal Of Engineering And Science*, vol. 4, no. 11, Nov. 2014.

[25] S. Devi and S. kaur, “Review Paper On Near Far Problem and Their Solution Technical,” *International Journal of Modern Computer Science (IJMCS)*, vol. 3, no. 2, Jun. 2015.

[26] S. Morshed and G. Heijenk, “Optimization and Verification of the TR-MAC Protocol for Wireless Sensor Networks,” *WWIC 2015: Wired/Wireless Internet Communications*, May. 2015.

[27] S. Morshed, M. Baratchi, and G. Heijenk, “Traffic-adaptive duty cycle adaptation in TR-MAC protocol for Wireless Sensor Networks,” *Wireless Days*, Mar. 2016.

[28] S. Morshed and G. Heijenk, “TR-MAC: An Energy-Efficient MAC Protocol Exploiting Transmitted Reference Modulation for Wireless Sensor Networks,” *MSWiM ’14 Proceedings of the 17th ACM international conference on Modeling, analysis and simulation of wireless and mobile systems.*, Jun. 2014.

[29] S. Morshed, M. Baratchi, P. K. Mandal, and G. Heijenk, “A Multi-channel Multiple Access Scheme Using Frequency Offsets - Modelling and Analysis,” *Wireless and Mobile Computing, Networking and Communications (WiMob).*, Dec. 2016.

[30] L. G. . Roberts, “Aloha Packet System With And Without Slots and Capture,” *ARPA Satellite System Note*, 1972.

[31] A. Varga, “Using the OMNeT++ discrete event simulation system in education,” *IEEE Transactions on Education*, vol. 42, no. 4, 1999.

[32] A. Köpke, M. Swigulski, K. Wessel, D. Willkomm, P. K. Haneveld, T. Parker, O. Visser, H. Lichte, and S. Valentin, “Simulating wireless and mobile networks in OMNeT++ the MiXiM vision,” in *Proceedings of the 1st international conference on Simulation tools and techniques for communications, networks and systems & workshops*, Marseille, France, Feb. 2008.

[33] A. Leong, D. Quevedo, and S.Dey, *Optimal Control of Energy Resources for State Estimation Over Wireless Channels*, ser. SpringerBriefs in Electrical and Computer Engineering. Springer International Publishing, 2017.

[34] H. Karl and A. Willig, *Protocols and Architectures for Wireless Sensor Networks*. Wiley, 2007.

[35] A. Goldsmith, *Wireless Communications*. Cambridge University Press, 2005.

[36] M. Safak, *Digital Communications*. Wiley, 2017.

[37] S. Y. Seidel and T. S. Rappaport, "914 MHz path loss prediction models for indoor wireless communications in multifloored buildings," *IEEE Transactions on Antennas and Propagation*, vol. 40, no. 2, pp. 207–217, Feb. 1992.